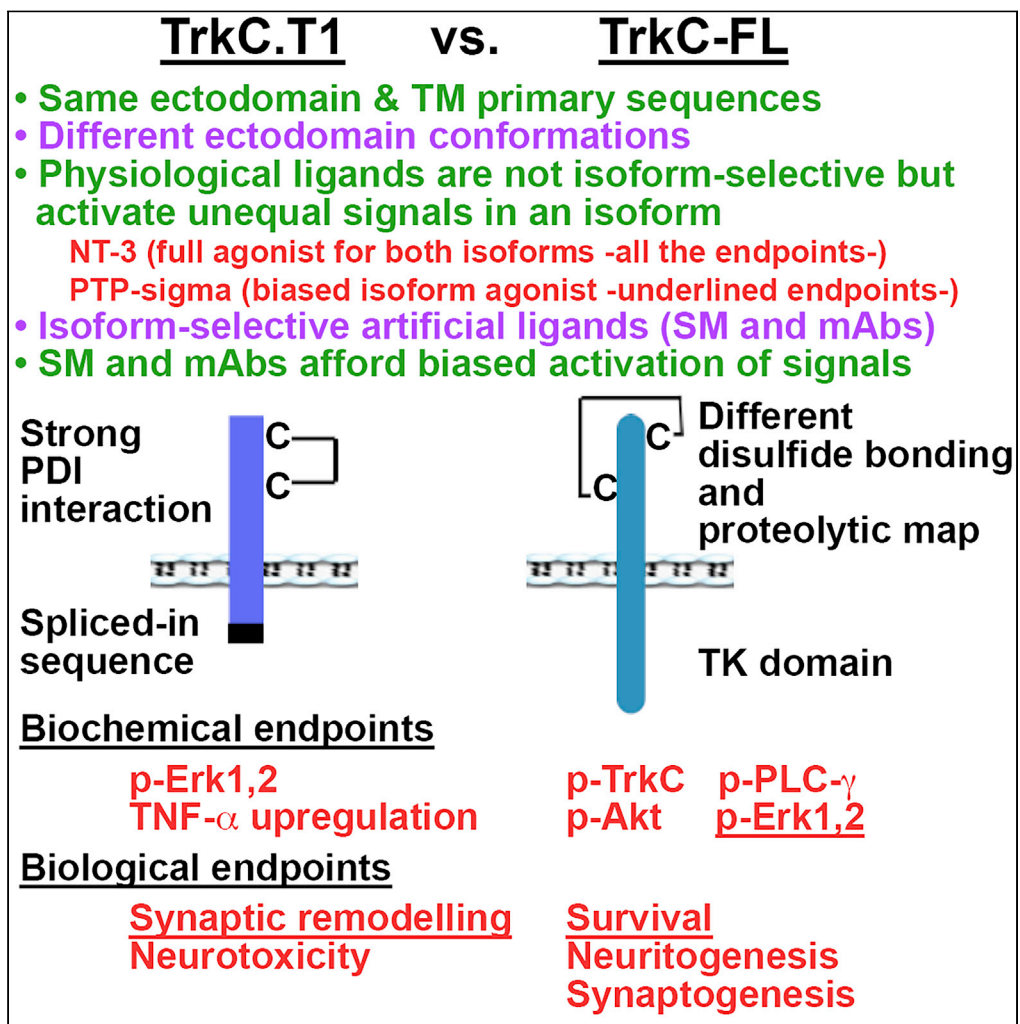


Article

Alternative Splicing of a Receptor Intracellular Domain Yields Different Ectodomain Conformations, Enabling Isoform-Selective Functional Ligands



Fouad Brahimi, Alba Galan, Sean Jmaeff, ..., Claudia L. Kleinman, David Y. Thomas, H. Uri Saragovi

uri.saragovi@mcgill.ca

HIGHLIGHTS

In transmembrane proteins the intracellular domain impacts the ectodomain conformation

Ectodomains with identical primary sequences can have different conformations

Native ligands can bind conformations non-selectively but activate in a biased manner

Synthetic ligands can bind and activate each receptor isoform selectively

Brahimi et al., iScience 23, 101447
September 25, 2020 © 2020 The Authors.
<https://doi.org/10.1016/j.isci.2020.101447>



Article

Alternative Splicing of a Receptor Intracellular Domain Yields Different Ectodomain Conformations, Enabling Isoform-Selective Functional Ligands

Fouad Brahim, ¹ Alba Galan, ¹ Sean Jmaeff, ^{1,4} Pablo F. Barcelona, ¹ Nicolas De Jay, ^{1,2} Kurt Dejgaard, ³ Jason C. Young, ³ Claudia L. Kleinman, ^{1,2} David Y. Thomas, ³ and H. Uri Saragovi ^{1,4,5,6,*}

SUMMARY

Events at a receptor ectodomain affect the intracellular domain conformation, activating signal transduction (out-to-in conformational effects). We investigated the reverse direction (in-to-out) where the intracellular domain may impact on ectodomain conformation. The primary sequences of naturally occurring TrkC receptor isoforms (TrkC-FL and TrkC.T1) only differ at the intracellular domain. However, owing to their differential association with Protein Disulfide Isomerase the isoforms have different disulfide bonding and conformations at the ectodomain. Conformations were exploited to develop artificial ligands, mAbs, and small molecules, with isoform-specific binding and biased activation. Consistent, the physiological ligands NT-3 and PTP-sigma bind both isoforms, but NT-3 activates all signaling pathways, whereas PTP-sigma activates biased signals. Our data support an “in-to-out” model controlling receptor ectodomain conformation, a strategy that enables heterogeneity in receptors, ligands, and bioactivity. These concepts may be extended to the many wild-type or oncogenic receptors with known isoforms.

INTRODUCTION

The TrkC receptor is a key player in the development, selection, maintenance, health, phenotype, and function of motor neurons, vascular endothelium, and other cell types (Saragovi et al., 2009; Segal, 2003; Sendtner et al., 1996; Youn et al., 2003). The *trkC* gene can generate, through alternative splicing, mRNAs encoding for several isoforms (Tsoulfas et al., 1993). The full-length TrkC (TrkC-FL) protein intracellular domain has a tyrosine kinase catalytic domain, whereas the truncated TrkC.T1 protein lacks the kinase and most of the intracellular domain but gains a new exonic sequence (Figure 1A). The *trkC* mRNA splicing event changes the primary sequence of the intracellular domain, but the juxtamembrane, the transmembrane, and the ectodomain primary sequences remain identical (Esteban et al., 2006). Both TrkC-FL and TrkC.T1 are naturally occurring, but their expression patterns differ in health and in disease, and more importantly the isoforms transduce opposite signals.

TrkC-FL is expressed throughout life, and the tyrosine kinase signals are key to maintaining motor neuron health, phenotype, and function (Deinhardt and Chao, 2014). TrkC.T1 is expressed embryonically and plays a role in development (Palko et al., 1999; Tessarollo et al., 1997). TrkC.T1 remains expressed in some healthy adult tissues, although generally at lower levels than TrkC-FL (Bai et al., 2010; Esteban et al., 2006). In healthy adult spinal cord and retina TrkC.T1 expression is very low, but in neurodegenerative diseases that affect these tissues the expression is significantly upregulated, at early stages of pathology (e.g., ALS, glaucoma, retinitis pigmentosa). TrkC.T1 plays a deleterious role by stimulating overproduction of TNF- α to neurotoxic levels, thus contributing to disease onset and progression (Bai et al., 2010; Brahim et al., 2016; Dorsey et al., 2006; Galan et al., 2017; Yanpallewar et al., 2012).

The primary amino acid sequence of TrkC-FL and TrkC.T1 ectodomains are identical, and both isoforms are bound by the same physiological ligands: the soluble growth factor NT-3 and the ectodomain of PTP-sigma expressed in an adjoining cell and binding in a heterotypic fashion. These ligands bind at non-overlapping receptor sites (D4-D5 and D1-D2 domains, respectively) and do not compete with each other (Coles et al., 2014; Takahashi et al., 2011). Similar high-affinity binding of NT-3 and PTP-sigma to the TrkC isoforms suggests highly conserved binding pockets.

¹Lady Davis Institute-Jewish General Hospital, McGill University, 3755 Côte St. Catherine, E-535, Montreal, QC H3T 1E2, Canada

²Department of Human Genetics, McGill University, Montreal, QC, Canada

³Department of Biochemistry, McGill University, Montreal, QC, Canada

⁴Department of Pharmacology, McGill University, Montreal, QC, Canada

⁵Department of Ophthalmology and Visual Science, McGill University, Montreal, QC, Canada

⁶Lead Contact

*Correspondence: uri.saragovi@mcgill.ca

<https://doi.org/10.1016/j.isci.2020.101447>



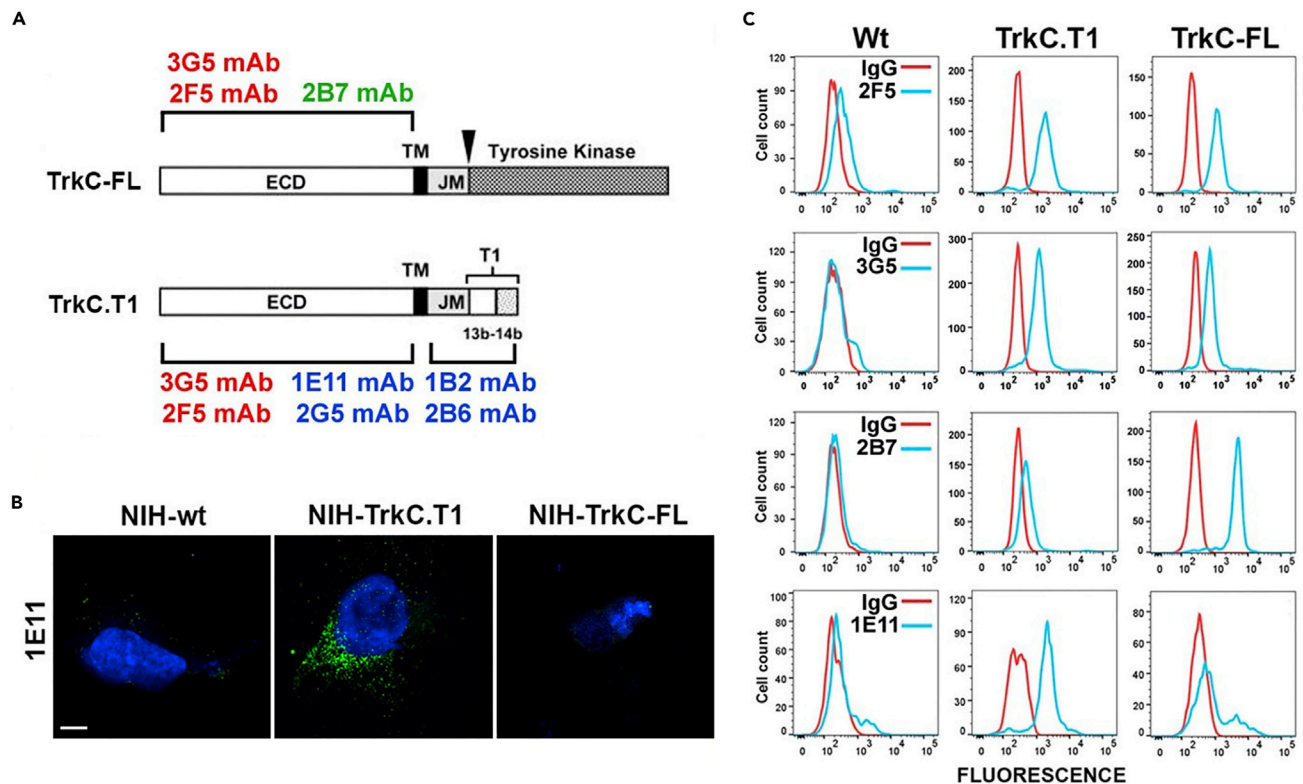


Figure 1. Binding of Isoform-Specific mAbs

(A) Schematic representation of the full-length TrkC (TrkC-FL) and truncated TrkC.T1 receptors. ECD, extracellular domain; TM, transmembrane domain; JM, intracellular juxtamembrane domain. MAbs binding to the ECD of both isoforms (red), the ECD of TrkC-FL only (green) or the ECD of TrkC.T1 only (blue), or the ICD of TrkC.T1 only (blue) are shown.

(B) Immunohistochemistry studies of wild-type or stably transfected NIH cells. Fluorescent microscopy shows that the mAb 1E11 bind to TrkC.T1 (green), and not to TrkC-FL expressing cells or to wild-type cells not expressing any TrkC isoform. Blue is nuclear staining using DAPI. Assays were repeated at least in three independent experiments, each in duplicate. Scale bar, 7 μ m.

(C) Cell surface receptors were studied by flow cytometry of live wild-type or stably transfected HEK293 cells, without permeabilization. MAbs 2F5 and 3G5 bind to both TrkC-FL and TrkC.T1, mAb 2B7 binds only to TrkC-FL, and mAb 1E11 binds only to TrkC.T1. Mouse IgG primary (red lines) is the background negative control. Assays were repeated at least in four independent experiments.

However, there are differences in how ligands can activate the isoforms. NT-3 activates the TrkC-FL kinase with sustained kinetics, to signal via pErk and pAkt, to promote cell survival and differentiation and activates TrkC.T1 via Arf6/Rac1 (Esteban et al., 2006) and pErk (Bai et al., 2010) to promote TNF- α production to neurotoxic levels (Brahimi et al., 2016; Galan et al., 2017). In contrast, PTP-sigma binding causes synaptic reorganization equally well through either isoform, and this function is independent of an intracellular domain or any known direct signal transduction (i.e., TrkC without any intracellular domain also promotes synaptic reorganization) (Coles et al., 2014; Takahashi et al., 2011). PTP-sigma has no other ascribed function via TrkC, and no cell survival or neuronal differentiation has been reported.

Thus, we hypothesized that NT-3 and PTP-sigma may activate other signals via each TrkC isoform and predicted that biased signals may be identified, binding TrkC with isoform target selectivity. Ligands with isoform selectivity would be desirable in neurodegenerative diseases to selectively activate TrkC-FL neuroprotection and to selectively inhibit TrkC.T1 neurotoxicity (Saragovi et al., 2019). However, designing or screening agents with isoform selectivity is challenging given the conserved primary sequences and conservation of the binding pockets of the natural ligands.

Here, we report the development of monoclonal antibodies (mAbs) and small molecules as artificial ligands that are isoform selective and act as biased agonists to activate in full certain signals. Using these chemical tools, we show that TrkC-FL and TrkC.T1 ectodomains have different conformations. We also demonstrate a mechanism that explains the different conformations or folding in the isoforms. TrkC.T1 associates with

protein disulfide isomerase (PDI), an enzyme that catalyzes different ectodomain disulfide bonding in TrkC.T1 compared with TrkC-FL.

The two different ectodomain conformations of TrkC-FL and TrkC.T1 are present *in vivo*, prompting the concept that the natural ligands NT-3 and PTP-sigma may functionally distinguish between these receptor conformations. NT-3 was confirmed as a full agonist for TrkC-FL (sustained kinetics, leading to survival and differentiation), whereas PTP-sigma acting via TrkC-FL is a biased agonist that transiently activates pErk1,2-mediated survival, without activating pAkt or cell differentiation. Moreover, NT-3 is an agonist of TrkC.T1-mediated promotion of TNF- α , whereas PTP-sigma does not activate this signal. This validates the concept that natural ligands binding either isoform can be functionally biased, a finding that is consistent with and validates physiologically the finding of artificial ligands (mAbs and small molecules) with biased function.

Together, the data support the concept that changes in the intracellular domain could affect the ectodomain conformation (“in-to-out” effects). This concept expands, in symmetric analogy, the established concept that ligand binding, or mutations, or protein-protein interactions at the ectodomain can affect the intracellular domain (“out-to-in” effects) (Changeux and Christopoulos, 2016; Dawson et al., 2005; Edelstein and Changeux, 2016; Lemmon et al., 2014). This in-to-out model may be expanded to other naturally occurring receptor isoforms or oncogenic receptors and may be used to identify isoform-selective naturally occurring or artificial biased functional ligands.

RESULTS

Ectodomain-Binding TrkC-FL-Specific or TrkC.T1-Specific mAbs

We reported a mAb 2B7 that binds selectively to the TrkC-FL ectodomain but binds poorly to the TrkC.T1 ectodomain (Brahimi et al., 2016). To study the molecular basis for binding selectivity, we generated additional mAbs that are selective for each isoform or for all isoforms (data are summarized in Figure 1A).

Immunohistochemistry (Figure 1B) and flow cytometry (Figure 1C) studies show that mAb 1E11 is preferentially selective for the TrkC.T1 ectodomain. The same results were obtained using the 2G5 mAb (data not shown). MAbs 2F5 and 3G5 are pan-TrkC mAbs and bind to both TrkC.T1 and TrkC-FL ectodomains and control for receptor expression (Figure 1C).

The mAb 2B7 epitope is at the linker region between D5 domain and the transmembrane domain, adjacent to D5 (Guillemard et al., 2010), the domain where NT-3 binds (Urfer et al., 1998). NT-3 (Kd 50 pM) blocks the binding of mAb 2B7 (Kd 2 nM) to TrkC-FL, but mAb 2B7 does not block the binding of NT-3 (Guillemard et al., 2010) (Szobota et al., 2019). NT-3 does not block binding of mAbs 1E11 and 2G5 to the TrkC.T1 ectodomain and does not block the binding of mAbs 2F5 and 3G5 to TrkC.T1 or TrkC-FL ectodomains.

These data indicate that it is possible to generate several mAbs that are isoform selective either for TrkC-FL or for TrkC.T1 ectodomains, even though the isoforms have the same primary sequence. In contrast, NT-3 binds to both receptor isoforms.

Other mAbs specific to the TrkC.T1 neopeptide intracellular domain (mAbs 1B2 and 2B6) (Figure S1) were made and used as further controls for TrkC.T1 expression. To evaluate the specific binding of the mAbs *in vivo*, spinal cord tissues where both TrkC isoforms are expressed were studied. Neurons express TrkC-FL but do not express TrkC.T1. Activated glia express TrkC.T1 mRNA at the onset of neurodegenerative diseases such as amyotrophic lateral sclerosis (ALS) (Brahimi et al., 2016), glaucoma (Bai et al., 2010), and retinitis pigmentosa (Galan et al., 2017). The TrkC.T1-specific mAbs were used to study protein expression in wild-type versus the SOD1 G93A mouse model of ALS in spinal cords *in vivo*.

In healthy mice there was low expression of TrkC.T1, but the protein was significantly increased in SOD1 G93A mice at the onset of ALS, co-localizing with GFAP⁺-activated glia and astrocytes. TrkC.T1 protein expression data are consistent with reports that TrkC.T1 mRNA expression in glia is associated with disease progression (Bai et al., 2010; Brahimi et al., 2016; Dorsey et al., 2006; Galan et al., 2017; Yanpallewar et al., 2012). These data demonstrate that the conformationally different ectodomains are present in tissue *in vivo* and further confirm the selectivity of mAb 1E11 (TrkC.T1 ectodomain binding) and mAb 1B2 (binding to the spliced-in neopeptide of the TrkC.T1 intracellular domain) (Figure S1).

Cysteine Modifications as the Basis for Ectodomain Conformational Differences and mAb Binding Specificity

The binding specificity of mAbs binding to TrkC ectodomains bearing identical primary sequence suggests differences in the ectodomain conformation. The presence of the full-length intracellular domain in TrkC-FL, the absence of most intracellular sequences in TrkC.T1, or the gain of the intracellular neoepitope in TrkC.T1 may be responsible.

We hypothesized that one possible conformational difference in the ectodomain may be at the disulfide bonds. Disulfide bonding is ultimately regulated by the entropy of the protein, and the distance of Cys residues, but alternate disulfide bonds can also form as intermediates during the folding process. In addition, endoplasmic reticulum (ER) enzymes such as PDI can break and reorganize disulfide bonding, until the final thermodynamically driven disulfide bonding configuration is achieved (Braakman and Hebert, 2013; Wallis and Freedman, 2013). ER transit time influences the ability of PDI to carry out disulfide reorganization of client proteins (Matsusaki et al., 2020).

We evaluated ER retention/export sequences (Geva and Schuldiner, 2014; Lee et al., 2004; Michelsen et al., 2005) in the intracellular domains of TrkC-FL and TrkC.T1 to potentially account for different ER transit times leading to different PDI interactions. The intracellular domain of TrkC-FL has seven ER export motifs and two ER retention motifs. The intracellular domain of TrkC.T1 has four ER retention motifs. An engineered construct deleting the whole intracellular domain (TrkC- Δ -ICD) has no intracellular ER retention/export motifs and serves as control (Figure S2).

From sequence analyses the prediction is that both TrkC-FL and TrkC- Δ -ICD transit rapidly through the ER and would have weak PDI associations, whereas TrkC.T1 transits more slowly through the ER and would have stronger PDI associations. This would result in TrkC-FL and TrkC- Δ -ICD adopting an intermediate disulfide bond pattern determined by kinetics, whereas TrkC.T1 would adopt a native thermodynamically driven PDI-mediated disulfide bond pattern and a different conformation (Kozlov et al., 2010b).

To evaluate this prediction, co-immunoprecipitations quantified the association of each TrkC isoform with PDI. TrkCT1, TrkC-FL, or TrkC- Δ -ICD was immunoprecipitated with anti-pan-TrkC (recognizing all isoforms), and samples were studied by western blotting using two different anti-PDI mAbs or two different anti-pan-TrkC mAbs (Figures 2A–2D).

PDI and TrkC.T1 are associated at a high ratio or at high stoichiometry, whereas PDI is associated with TrkC-FL or with TrkC- Δ -ICD at a significantly lower level (Figure 2A). When standardized to the total TrkC loaded in each lane, TrkC.T1 has a 4-to 6-fold higher associated PDI than the other two isoforms (Figure 2B).

Analyses of the samples under non-reducing conditions demonstrate that the majority of the PDI•TrkC.T1 is detected as a complex, at a mass above 245 kDa (Figure 2C left panel). This is consistent with the reaction mechanism of PDI (Kozlov et al., 2010a) in which it forms transient disulfide bonds with substrates (Braakman and Hebert, 2013). A minority of the associated PDI•TrkC.T1 is non-covalent or of low stoichiometry, and a ladder of free PDI protein is also detected (Figure 2C right panel).

In contrast, PDI•TrkC-FL and PDI•TrkC- Δ -ICD association is mostly non-covalent; these TrkC isoforms are detected in their free state under non-reducing conditions. Very low levels of PDI•TrkC-FL and PDI•TrkC- Δ -ICD are detected as a stable complex, at a mass above 245 kDa (Figure 2C left panel). The Mr heterogeneity of the TrkC isoforms is expected from their different intracellular domain mass (Figures 2A and 2C).

Consistent with our predictions that TrkC-FL and the TrkC- Δ -ICD isoforms share a related conformation, mAb 2B7 binds to both TrkC-FL and TrkC- Δ -ICD but less efficiently to TrkC.T1. These data suggest and that TrkC.T1 conformation is different from that of TrkC-FL and TrkC- Δ -ICD.

To evaluate this concept, we tested whether mAb 2B7 binding is sensitive to mild reducing agents. In flow cytometry assays using live cells, mild reduction of TrkC.T1 results in gain of mAb 2B7 binding at the cell surface (Figure 2D). This shows that breaking at least some of the disulfide bonds in TrkC.T1 unmask the 2B7 epitope and supports the view that TrkC.T1 has a different disulfide configuration. Western blot analyses support a similar conclusion, as mild reduction of TrkC.T1 (without full denaturation of the sample)

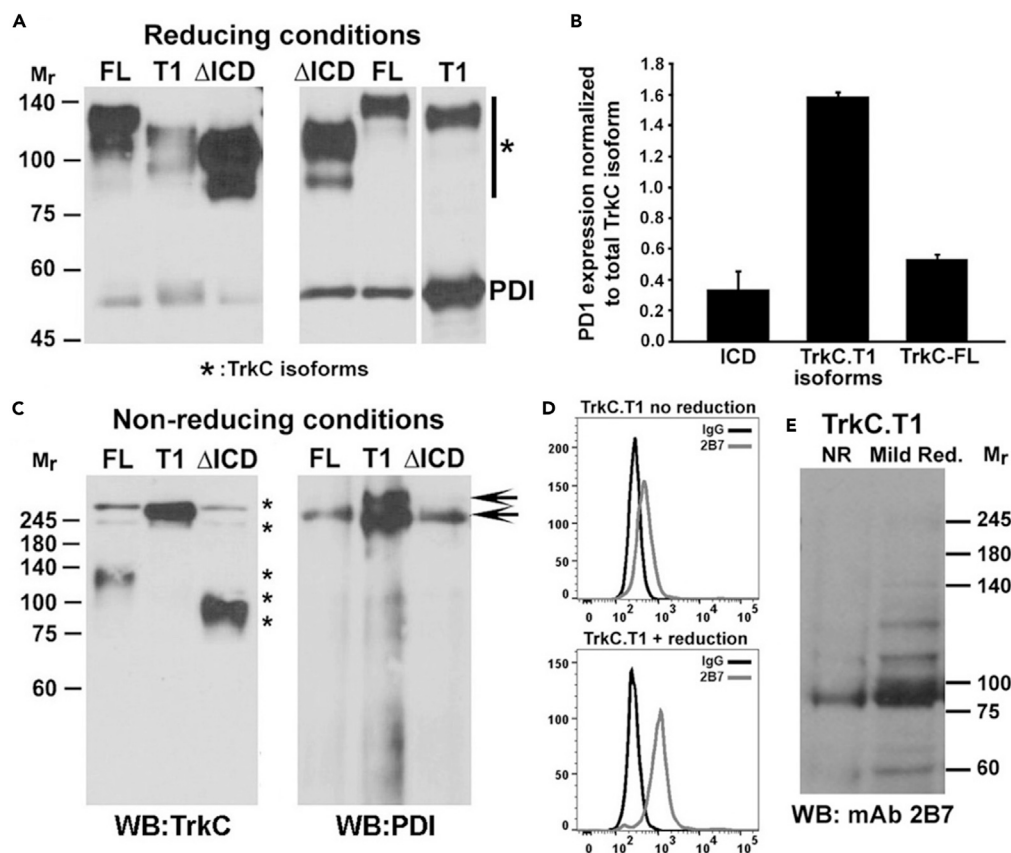


Figure 2. TrkC Isoforms Have Different Disulfide Bonding and Association with PDI

All assays were repeated at least in three independent experiments.

(A) Co-immunoprecipitation of PDI with TrkCT1 or TrkC-FL or TrkC-Δ-ICD HEK293 lysates. Immunoprecipitations using a pan-TrkC antibody were resolved by SDS-PAGE under reducing conditions, and membranes were immunoblotted with anti-pan-TrkC (C44H5) or with anti-PDI mAbs (results were replicated using two different anti-PDI mAbs). The different Mr of each TrkC isoform is due to the length of the ICDs. Heterogeneity is due to glycosylation. Left panel, same cell lysate equivalents loaded. Right panel, same TrkC levels loaded.

(B) Quantification of PDI/TrkC ratios. TrkC.T1 associates with PDI at a high ratio or stoichiometry, approximately four times higher than the other isoforms. Data are mean ± standard deviation.

(C) TrkC immunoprecipitates were resolved in non-reduced SDS-PAGE and immunoblotted with a pan-TrkC antibody or anti-PDI mAbs. Almost all the TrkC.T1 is in a high-molecular-weight complex co-migrating with PDI.

(D) Flow cytometry show that TrkC-FL-specific 2B7 mAb does not bind to cell surface TrkC.T1 (top), but cell surface TrkC.T1 binding is gained (bottom) after exposing live cells to mild reduction.

(E) Western blots of whole-cell lysate samples show that TrkC-FL-Δ-ICD specific 2B7 mAb does not bind to non-reduced TrkC.T1 (NR), but binding is gained after mild reduction of cell lysates.

results in increased mAb 2B7 binding to TrkC.T1 (Figure 2E). The flow cytometry and western blot assays are consistent in that mild reduction significantly enhances mAb 2B7 binding to TrkC.T1.

Conformational Differences in the Ectodomains of the Isoforms

Immunoprecipitations of TrkC isoforms (using a pan-TrkC mAb) were subjected to trypsin peptide mapping and studied by liquid chromatography-mass spectrometry (LC/MS). The same samples were studied under reducing and non-reducing conditions, to detect tryptic fragments that remain paired under non-reducing conditions. The datasets were analyzed using bioinformatic tools (Scaffold 4.8.9).

The peptide maps for the TrkC-FL and TrkC-Δ-ICD isoforms are similar, suggesting a similar conformation. TrkC-FL and TrkC-Δ-ICD isoforms displayed a variety of intra-chain disulfide bonds. However, their map differs significantly from the map of the TrkC.T1 isoform (Figure 3). Notably, after digestion TrkC.T1 is

TrkC-FL

MDVSLCPAK | CSFWR | IFLGSLVLDYVGSVLA^CPANCV^CSK | TEINCR | RPDDGNLPLEGGQDSGNSNGNASINITDISR | NITSIHIENWR | **SLHTLNAVDMELYTGLQK** | LTIK | NSGLR | SIQPR | AFAKNPHLR | **YINLSSNR** | **LTTL^WQLFQ^TLSLR** | ELQLEQNFNCSCDIR | **WMQLWQEQQEAK** | LNSQNL^YCINADGSQ^LPLFR | MNISQ^CDLPEISVSHVNLTVR | EGDNAVIT CNGSGSPLPDVDWIVTGLQSINTHQ^TNLNWTVNHAINLTLVNVTS^EDNGF^TLT CIAENVVGM^SNASVALTVY^YPPR | **VVSLE EPELR** | LEHCIEFVVR | **GNPPPTLHWLHNGQPLR** | ESKI IHVEYYQEGEISEG^CLLENK^PTHYNNGN^YT^LIAKNPLGTANQT INGHFLKEPFPESTDNFI^LFDEVSP^TPPITV^TTHKP | EEDT

TrkC-Δ-ICD

MDVSLCPAK | CSFWR | IFLGSLVLDYVGSVLA^CPANCV^CSK | TEINCR | RPDDGNLPLEGGQDSGNSNGNASINITDISR | **NITSIHIENWR** | **SLHTLNAVDMELYTGLQK** | **LTIK** | NSGLR | SIQPR | AFAKNPHLR | **YINLSSNR** | **LTTL^WQLFQ^TLSLR** | ELQLEQNFNCSCDIR | **WMQLWQEQQEAK** | LNSQNL^YCINADGSQ^LPLFR | MNISQ^CDLPEISVSHVNLTVR | EGDNAVIT CNGSGSPLPDVDWIVTGLQSINTHQ^TNLNWTVNHAINLTLVNVTS^EDNGF^TLT CIAENVVGM^SNASVALTVY^YPPR | **VVSLE EPELR** | LEHCIEFVVR | **GNPPPTLHWLHNGQPLR** | ESKI IHVEYYQEGEISEG^CLLENK^PTHYNNGN^YT^LIAKNPLGTANQT INGHFLKEPFPESTDNFI^LFDEVSP^TPPITV^TTHKP | EEDT

TrkC-T1

MDVSLCPAK | CSFWR | IFLGSLVLDYVGSVLA^CPANCV^CSK | TEINCR | RPDDGNLPLEGGQDSGNSNGNASINITDISR | NITSIHIENWR | **SLHTLNAVDMELYTGLQK** | LTIK | NSGLR | SIQPR | AFAKNPHLR | **YINLSSNR** | **LTTL^WQLFQ^TLSLR** | ELQLEQNFNCSCDIR | **WMQLWQEQQEAK** | LNSQNL^YCINADGSQ^LPLFR | MNISQ^CDLPEISVSHVNLTVR | EGDNAVIT CNGSGSPLPDVDWIVTGLQSINTHQ^TNLNWTVNHAINLTLVNVTS^EDNGF^TLT CIAENVVGM^SNASVALTVY^YPPR | **VVSLE EPELR** | LEHCIEFVVR | **GNPPPTLHWLHNGQPLR** | ESKI IHVEYYQEGEISEG^CLLENK^PTHYNNGN^YT^LIAKNPLGTANQT INGHFLKEPFPESTDNFI^LFDEVSP^TPPITV^TTHKP | EEDT

Figure 3. TrkC Isoforms Have Different Disulfide-Bonding Patterns

HEK293 lysates expressing TrkC isoforms were immunoprecipitated using a pan-TrkC mAb and the proteins were digested with trypsin. Samples were studied by LC/MS, with half of each sample first subjected to reduction/alkylation of S-S bonds (half of each sample was not). **Red letters**: peptides detected under reducing conditions only. **Blue letters**: peptides detected under both reducing and non-reducing conditions. Dashed vertical lines: trypsin cut sites. Cysteines are underlined in gray. The fragmentation patterns of TrkC-FL and TrkC-Δ-ICD are highly related and very different from the fragmentation pattern of TrkC.T1.

the only isoform where homodimer fragments are detected (LTTL^WQLFQ^TLSLR fragment), under non-reducing conditions, although they contain no cysteines. This suggests that in TrkC.T1 the fragments remain aggregated. These data indicate that the conformation of the TrkC-FL and TrkC-Δ-ICD isoforms is different from that of TrkC.T1 and that the disulfide bonds are different.

Overall, the data in Figures 2 and 3 confirm that each TrkC isoform has a distinct conformation, disulfide bonding, and PDI association and indicate that splicing of the intracellular domain can cause conformational differences at the ectodomain. The data in Figure 1 support this conclusion. Although the receptor isoforms have an identical primary amino acid sequence, and the natural ligand NT-3 does not discriminate between isoforms, structural differences may be exploited to generate isoform-selective ligands.

Ectodomain-Binding Isoform-Specific mAbs Can Be Agonistic

Next, we tested the isoform-specific mAb ligands for activation of signal transduction in assays quantifying cell survival and differentiation (TrkC-FL function) and stimulation of TNF-α production (TrkC.T1 function) (Brahimi et al., 2016). NT-3 is a non-discriminating agonist of both isoforms and serves as positive control.

NT-3 activates cell survival and cell differentiation. MAb 2B7 activates TrkC-FL to promote cell survival with maximal efficacy similar to NT-3 (Figure 4A) but does not promote cellular differentiation (Guillemand et al., 2010). Therefore, mAb 2B7 is a biased agonist for TrkC-FL isoforms. In addition, mAb 2B7 does not activate TrkC.T1 and does not induce TNF-α (Figure 4B) (as expected because it does not bind cell surface TrkC.T1). In sum, mAb 2B7 is a TrkC-FL-specific agonist biased to cell survival and it is more receptor specific than NT-3 because it does not bind to TrkC.T1 (Brahimi et al., 2016) or p75NTR (Guillemand et al., 2010).

MAb 2F5 binds to both TrkC-FL and to TrkC.T1 and functionally is an agonist for both isoforms. MAb 2F5 promotes limited cell survival with significantly lower efficacy than NT-3 (Figure 4A) but promotes TNF-α production to levels similar to NT-3 (Figure 4B). The effective molar concentration for mAb 2F5 is the same for each isoform, indicating equivalent potency. However, relative to NT-3, mAb 2F5 activates the

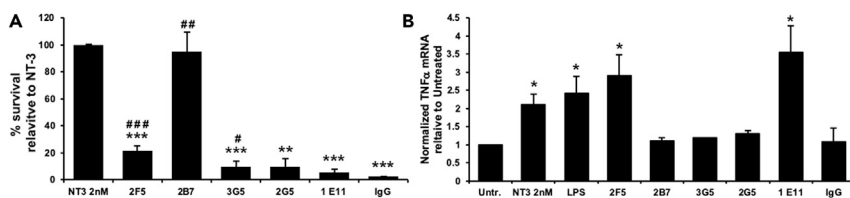


Figure 4. Isoform-Selective mAb Ligands Have Isoform-Selective Bioactivity

All assays were repeated at least in three independent experiments, each in triplicate. Dose-responses not shown, for simplicity (for further information see Figure S5). Data are mean \pm standard deviation. One symbol $p < 0.05$, two symbols $p < 0.01$, three symbols $p < 0.001$.

(A) HEK293 cells expressing TrkC-FL receptors were cultured in serum-free media (to induce death) and were supplemented with the indicated ligands (40 nM for mAbs, 2 nM for NT-3). Cell survival was determined after 72 h by MTT colorimetric assays (similar results were obtained after 48 h, not shown). Untreated (vehicle) and mouse IgG are controls (0% survival), NT-3 at the optimal 2 nM dose is set to 100% survival. The symbol # shows significance versus mouse IgG control. The symbol * shows significance versus NT-3 positive control. MAb 2B7 significantly promotes cell survival, to levels similar to NT-3. MAbs 2F5 and 3G5 also promote cell survival but to a lower degree than NT-3. MAbs 2G5, and 1E11 do not promote cell survival and are not different from mouse IgG control (one-way ANOVA with Tukey-Kramer multiple comparisons).

(B) TNF- α mRNA quantified by quantitative real-time PCR after 6 h of treatment in glial rMC-1-TrkC.T1. The values were standardized to the vehicle control (untreated, set to 1). NT-3 (2 nM) and LPS (1 μ g/mL) are positive controls. MAbs (at 40 nM) 2F5 and 1E11 significantly increase TNF- α mRNA levels (* $p < 0.05$ versus untreated or mouse IgG controls). The mAbs 2B7, 3G5, and 2G5 do not increase TNF- α and are not different from untreated or mouse IgG controls (two-tailed t test).

TrkC.T1 isoform with higher efficacy. MAb 3G5 also binds to both TrkC-FL and TrkC.T1 and promotes limited cell survival via TrkC-FL, without promoting TNF- α production via TrkC.T1. Hence the mAbs can be partial agonists and they can activate the isoforms asymmetrically in spite of comparable binding to both isoforms.

MAb 1E11 is TrkC.T1 specific and activates TrkC.T1 with high efficacy, inducing TNF- α production to levels similar to control NT-3 or control LPS (Figure 4B). Silencing TrkC.T1 mRNA expression (using pLKO-1 viral vectors expressing shRNA (Brahimi et al., 2016) prevents TNF- α induction by mAb 1E11 and by NT-3 but does not prevent TNF- α induction by LPS control (Figure S3). These data demonstrate that TNF- α production is dependent on TrkC.T1 expression and is ligand dependent. In cellular controls, the TrkC.T1-specific mAb 1E11 does not promote cell survival through TrkC-FL (Figure 4A), as expected because it does not bind this isoform. Hence mAb 1E11 is a TrkC.T1-specific agonist.

Ectodomain-Binding Isoform-Specific Small Molecules Can Be Agonistic

To expand the proof of concept of isoform-selective agonistic ligands, we studied small molecules (3Aa and 1Aa) and their labeled analogs (3Aa-FITC and 1Aa-FITC, containing a fluorescein label). We previously reported in quantitative flow cytometry assays that 3Aa and 1Aa are ligands binding to the TrkC-FL ectodomain. Small molecule TrkC ligands had not been evaluated for isoform specificity, because at the time the concept of different isoform structures and differential ligand binding had not been rationalized.

Here, we demonstrate isoform specificity by small molecule TrkC ligands 3Aa and 1Aa, in terms of receptor binding (Figures 5A and 5B) and in terms of receptor activation (Figures 5C–5E).

In immunohistochemistry assays (Figure 5A) and in quantitative flow cytometry assays (Figure 5B) 3Aa-FITC binds to cells expressing TrkC-FL but it does not bind to cells expressing TrkC.T1 above the background of control wild-type cells not expressing any TrkC isoforms. Previous work showed that 3Aa-FITC does not bind to other Trk-receptor family members (Zaccaro et al., 2005); hence, 3Aa binds with TrkC-FL isoform specificity, and such selectivity is remarkable for a small molecule. In contrast, 1Aa-FITC binds to both TrkC isoforms (Table 1).

Biological assays evaluated cell differentiation and cell survival signals in TrkC-FL-expressing cells. Treatment with 3Aa and 1Aa induces significant cellular differentiation to levels comparable with NT-3 (Figure 5C), but with lower potency (10–50 μ M for small molecules versus 0.2–2 nM for NT-3). 3Aa and 1Aa also promote low but significant survival compared with untreated control cultures (Figure 5D) as reported

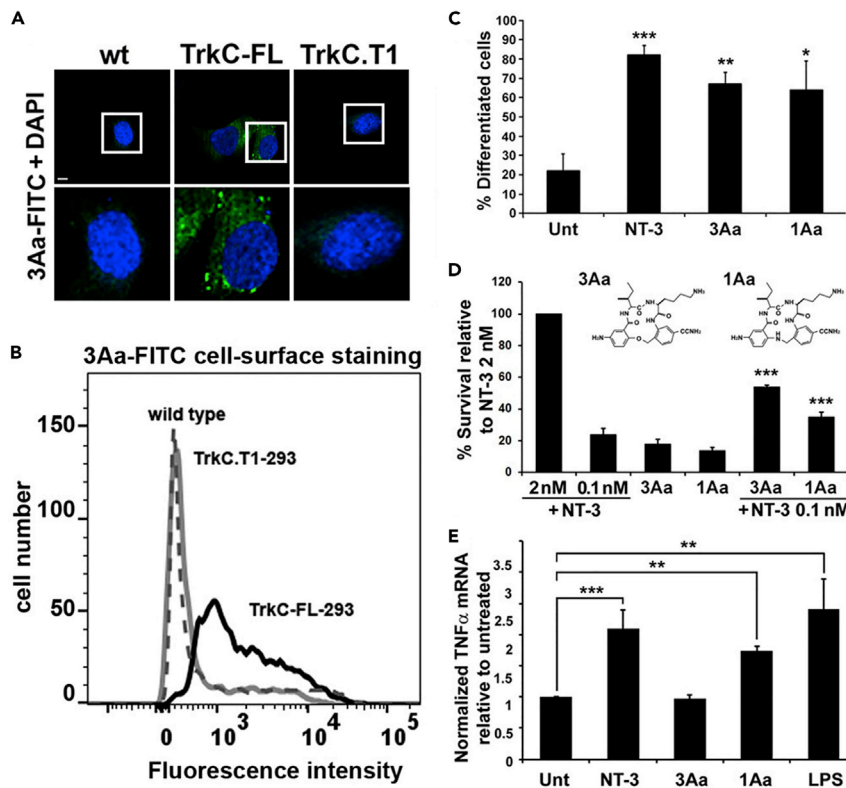


Figure 5. Binding and Bioactivity of Isoform-Specific Small Molecule Ligands

All assays were repeated at least in three independent experiments, each in triplicate. Data are mean \pm standard deviation. Symbols indicate significance *** p < 0.001, ** p < 0.01, * p < 0.05 (two-tailed t test). The binding and bioassays shown for **3Aa** and **1Aa** are at 10 μ M (as per Zaccaro et al., 2005). Optimal NT-3 is 2 nM, and 0.1 nM NT-3 is suboptimal (for dose-dependent bioassay data see Figure S5).

(A) Binding assays by immunohistochemistry in HEK293 cells. Merged DAPI and FITC channels are shown. The bottom panels show a higher magnification of the top panel areas within the white rectangles. Scale bar, 7 μ m. Fluorescein-conjugated **3Aa** (**3Aa-FITC**) binds predominantly to TrkC-FL and binding is lower or undetectable to TrkC.T1.

(B) Binding assays by quantitative flow cytometry. Ligand binding to the cell surface, using live, non-permeabilized HEK293 cells. **3Aa-FITC** binds to TrkC-FL.

(C) Biological assays of cell differentiation via TrkC-FL. **3Aa** and **1Aa** induce differentiation of nnr5-TrkC-FL cells, to levels similar as 2 nM NT-3 control. Differentiation was determined as percentage of cells with neurites (defined as length >2 cell bodies). Significance shown is versus untreated.

(D) Biological assays of cell survival via TrkC-FL. **3Aa** and **1Aa** promote the survival of HEK293-TrkC-FL cells induced to die by culture in serum-free media. Data are standardized to 2 nM NT-3 100% survival, and untreated 0% survival. **3Aa** and **1Aa** can potentiate the suboptimal action of 0.1 nM NT-3 (*** p < 0.001 significance versus 0.1 nM NT-3 control). For simplicity, some statistics are not shown in the graph: (i) all agents are significant versus untreated, (ii) the survival promoted by **3Aa** and **1Aa** is not different from suboptimal 0.1 nM NT-3 but is significantly lower than optimal 2 nM NT-3. Structures of **3Aa** and **1Aa** are shown.

(E) Biological assays of TNF- α induction via TrkC.T1. **1Aa** induces TNF- α mRNA, similar to controls NT-3 (2 nM) or LPS (1 μ g/mL). In contrast, **3Aa** does not induce TNF- α mRNA, as expected since it does not bind efficiently to TrkC.T1 (see A and B).

(Zaccaro et al., 2005). In addition, **3Aa** and **1Aa** potentiate the action of 0.1 nM NT-3 (*** p < 0.001 significance versus each ligand alone).

In sum, **3Aa** and **1Aa** are TrkC-FL partial agonist small molecules with biased signaling. They promote TrkC-FL function of cell survival with low efficacy and TrkC-FL function of cellular differentiation with good efficacy. However, their potency is low and activity requires relatively high concentrations.

The small molecules were then evaluated for TrkC.T1 signaling. Biological assays show that **3Aa** does not activate TrkC.T1, as expected, since **3Aa** does not bind to TrkC.T1. On the other hand, **1Aa** activates

Fold-Increase in Ligand Binding over Controls			
	Ligand	TrkC-FL	TrkC.T1
Not Isoform Selective			
1	NT-3	9	7
2	2F5 mAb	7.2	7.4
3	3G5 mAb	3	4.4
4	1Aa	6	5
5	PTP-sigma	5	3.7
Selective TrkC-FL			
6	2B7 mAb	16.3	–
7	3Aa	12	–
Selective TrkC.T1			
8	1E11 mAb	1.3	11.5
9	2G5 mAb	–	14

Table 1. Summary of TrkC Ligands Binding at the Ectodomain

Quantitative flow cytometry assays of ligand binding at the cell surface of cells stably transfected to express TrkC-FL or TrkC.T1. The data are fold-increase in mean fluorescence intensity (average $n \geq 3$) over all controls. Controls used are wild-type cells (untransfected), non-binding IgG, and labeled small molecule analogs that bind other targets. Data exemplified in Figures 1C and CS4 and previous work (Zaccaro et al., 2005). Binding is done at ligand-saturation concentrations, under conditions that yield low non-specific background staining, and high signal/noise ratios.

NT-3 binds to both isoforms. PTP-sigma binds to both isoforms. 2F5 and 3G5 mAbs bind both isoforms. 1E11 and 2G5 mAbs bind selectively to TrkC.T1, and mAb 2B7 binds selectively to TrkC-FL. Small molecule 3Aa binds TrkC-FL (this paper and Zaccaro et al., 2005) but does not bind to TrkC.T1. In contrast, small molecule 1Aa binds to TrkC-FL (this paper and Zaccaro et al., 2005) and also to TrkC.T1. Not listed are mAbs 1B2 and 2B6 that bind selectively to the intracellular neopeptide of TrkC.T1.

NT-3-biotin was detected using avidin-fluorescein secondary. 1Aa and 3Aa were directly labeled by conjugation with fluorescein (1:1 fluorescein-per molecule). Mouse mAbs were detected using anti-mouse secondary. PTP-sigma was detected using anti-human secondary. Differences in the absolute fluorescence intensity can be ascribed to the different number of fluorescein conjugates and to different signal amplification and the stoichiometry of multiple secondary binding to a primary.

TrkC.T1 to induce TNF- α production to levels comparable with that of control NT-3 (Figure 5E). Therefore, functionally 3Aa is a TrkC-FL-specific agonist, whereas 1Aa is an agonist that is not isoform specific.

It is somewhat surprising that 3Aa and 1Aa have different isoform selectivity, because they have a closely related chemical structure with the only difference being that one has an amine and the other an ether in the ring (Figure 5D). Isoform selectivity and structure-activity relationship studies for >50 small molecule TrkC ligands (Brahimi et al., 2010; Chen et al., 2009; Zaccaro et al., 2005) will be reported elsewhere.

Isoform binding and functional selectivity achieved with artificial ligands (mAbs and small molecules) further supports the notion that there are structural differences in the receptors despite their invariant primary sequence. Structural differences suggest a refined control of receptor activation, which would seem necessary to maintain normal physiology, especially given that the natural ligand NT-3 can activate both isoforms.

A Non-neurotrophin Endogenous Ligand Functionally Interacts with TrkC Isoforms in a Biased Manner

The ectodomain of PTP-sigma is reported to bind to TrkC-FL and TrkC.T1 and to promote synaptic reorganization. Synaptic reorganization induced by PTP-sigma was mediated also by TrkC- Δ -ICD, indicating that the effect is independent of any TrkC intracellular domain and of any reported TrkC-signal transduction (Coles et al., 2014; Takahashi et al., 2011).

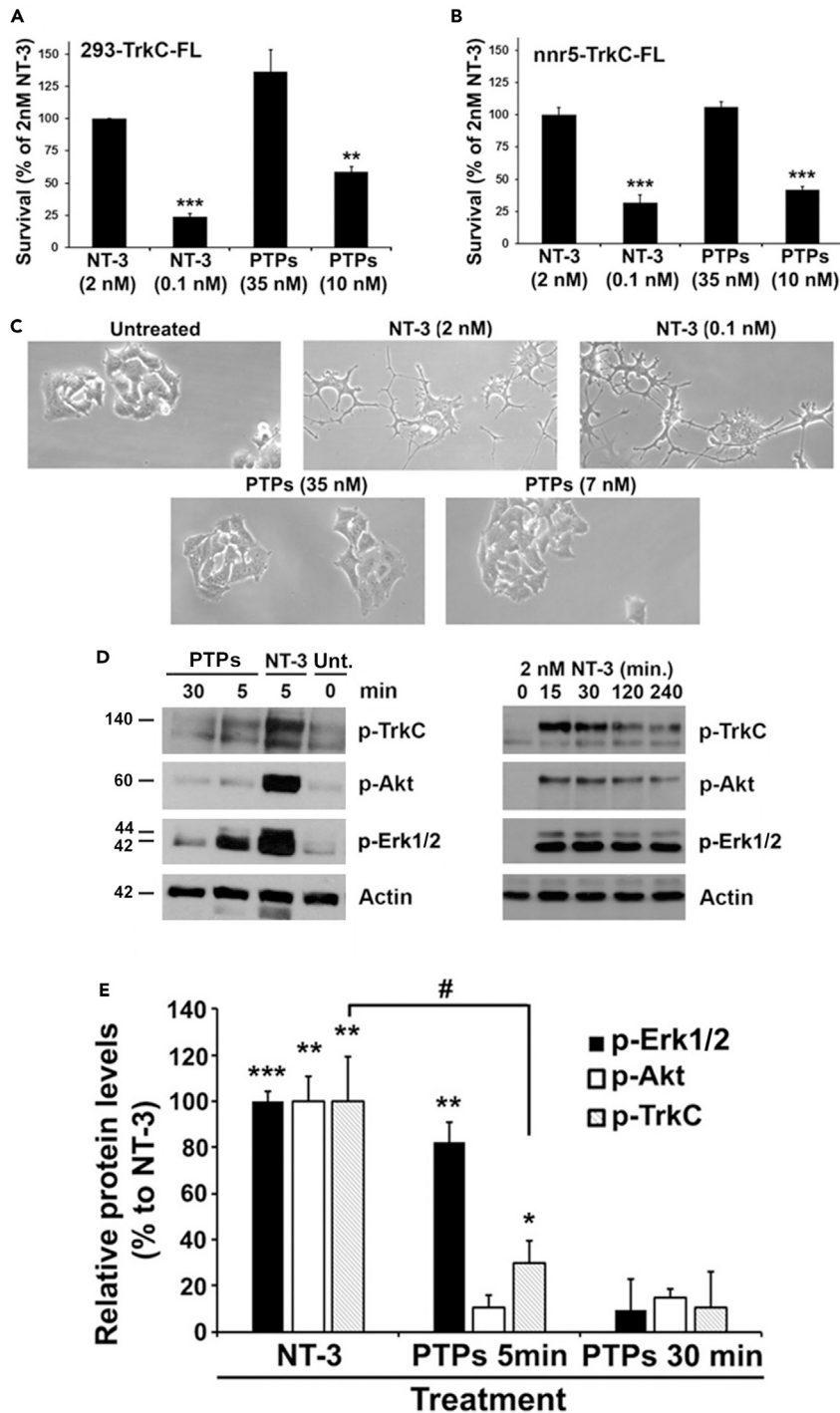


Figure 6. Biased Agonism by a Non-Neurotrophin Endogenous Ligand of TrkC-FL, the Ectodomain of PTP-Sigma

PTP-sigma ectodomain binds to all TrkC isoforms (Figure S4) and was evaluated for bioactivity via TrkC-FL. Data are standardized to 2 nM NT-3 = 100% survival, untreated = 0% survival.

(A) PTP-sigma promotes the survival of 293-TrkC-FL cells induced to die by culture in serum-free media. PTP-sigma (35 nM optimal dose) is as effective as NT-3 (2 nM optimal dose), but dose-dependent studies show that in this biological endpoint it is 20- to 50-fold less efficient than NT-3 (significance versus optimal NT-3). Data are mean \pm standard deviation. Symbols indicate significance *** $p < 0.001$, ** $p < 0.01$; two-tailed t test). Similar data were obtained using NIH3T3-TrkC-FL cells.

Figure 6. Continued

(B) PTP-sigma and NT-3 promote the survival of nnr5-TrkC-FL cells (a PC12 cell variant, expressing TrkC-FL and p75^{NTR}). The effect of PTP-sigma and NT-3 is dose dependent (significance versus optimal NT-3, ***p < 0.001; two-tailed t test). (C) In spite of promoting survival signals, PTP-sigma binding does not promote any cell differentiation or neuritic outgrowth in nnr5-TrkC-FL cells, whereas differentiation is clearly promoted by NT-3. (D) Biochemical signals in HEK293-TrkC-FL cells (n = 3 independent assays). The PTP-sigma signal is transient and decreases to baseline by 30 min, whereas the NT-3 signal is sustained for hours. p-Erk1,2 is significantly stimulated by PTP-sigma and is not statistically different from NT-3 at the 5-min time point. (E) Quantification showing significance versus baseline (***p < 0.001, **p < 0.01, or *p < 0.05; one-way ANOVA with Tukey-Kramer multiple comparisons). The pTrkC signal is also activated transiently at the 5-min time point, to a significantly lower degree than NT-3 (#p < 0.05).

To understand the PTP-sigma signaling mechanisms, we evaluated binding and activation for each TrkC isoform. In flow cytometry assays using live cells, the ectodomain of PTP-sigma ectodomain binds to all cell surface TrkC isoforms (Figure S4) as reported by others (Coles et al., 2014; Takahashi et al., 2011). Hence, PTP-sigma binding is impervious to the different conformation of each TrkC ectodomain. Moreover, PTP-sigma (Kd 9.3 ± 1.2 nM) and NT-3 do not cross-compete each other's binding (Coles et al., 2014; Takahashi et al., 2011), and this is consistent with PTP-sigma binding at the D1/D2 domains (Coles et al., 2014; Takahashi et al., 2011), whereas NT-3 binds at the D5 domain (Urfer et al., 1995, 1998).

In biological assays using TrkC-FL-expressing cells stressed by culture in serum-free media, PTP-sigma promotes cell survival. In these assays, 35 nM PTP-sigma induces a maximal survival that is similar to optimal 2 nM NT-3 control. Although the efficacy of PTP-sigma is equal to NT-3, on a molar basis PTP-sigma is 20- to 50-fold less potent than NT-3 (Figures 6A and S5). The efficacy and potency of PTP-sigma at promoting cell survival via TrkC-FL is the same whether or not cells co-express the NT-3 co-receptor p75^{NTR} (Figure 6B). However, PTP-sigma acting through TrkC-FL does not promote cellular differentiation whatsoever (Figure 6C).

The biological endpoints triggered by PTP-sigma binding to TrkC-FL are associated with signal transduction that is biased to pErk1,2 (Figure 6D, quantified in 6E). Compared with NT-3, PTP-sigma activates pErk1,2 signals to a maximal level that is not different from NT-3. However, the PTP-sigma signals are transient and last 5–7 min, whereas NT-3 signals are sustained for hours (Guillemard et al., 2010; Ivanisevic et al., 2003). Moreover, PTP-sigma also transiently activates pTrkC signals significantly over vehicle control, but to a significantly lower degree than NT-3.

The kinetics of the biochemical signals induced by PTP-sigma in TrkC-FL-expressing cells are consistent with promotion of survival without promotion of differentiation (Saragovi et al., 1998; Zhang et al., 2000). Ligand-induced receptor internalization may be relevant to these biological signals (Saragovi et al., 1998). The pErk-biased signal transduction of PTP-sigma is analogous to mAb 2B7 (Brahimi et al., 2016), a ligand which also induces cell survival but not differentiation (Guillemard et al., 2010). However, there are differences between PTP-sigma and mAb 2B7 in that the latter induces pErk-activation with sustained kinetics, more similar to NT-3 kinetics.

In biological assays using TrkC.T1-expressing cells, PTP-sigma does not promote activation of pErk (Figure 7A) and does not promote TNF- α production (Figure 7B). In contrast, the positive control NT-3 activates pErk and promotes TNF- α production as an agonist of TrkC.T1.

These biochemical and biological endpoints are dependent on TrkC.T1 expression, because silencing TrkC.T1 prevents NT-3-induced pErk and TNF- α production (Figure S3). Consistent with this control, we had previously reported that silencing TrkC.T1 expression or inhibiting TrkC.T1 activation prevents TNF- α over-production and neurodegeneration *in vivo* (Galan et al., 2017).

Hence, PTP-sigma is not an agonist for the TrkC.T1-mediated endpoints of pErk activation (biochemical signals) and promotion of TNF- α production (biological signals), even though it binds to this isoform. The identification of a biased natural ligand PTP-sigma that functionally discriminates between TrkC isoforms provides a physiological counterpart to the isoform-selective TrkC artificial ligands (mAbs and small molecules).

In sum, NT-3 binds both isoforms and is a full agonist for both isoforms, whereas PTP-sigma binds both isoforms but functionally is a biased agonist in terms of receptor selectivity (only TrkC-FL activation) as well as in terms of

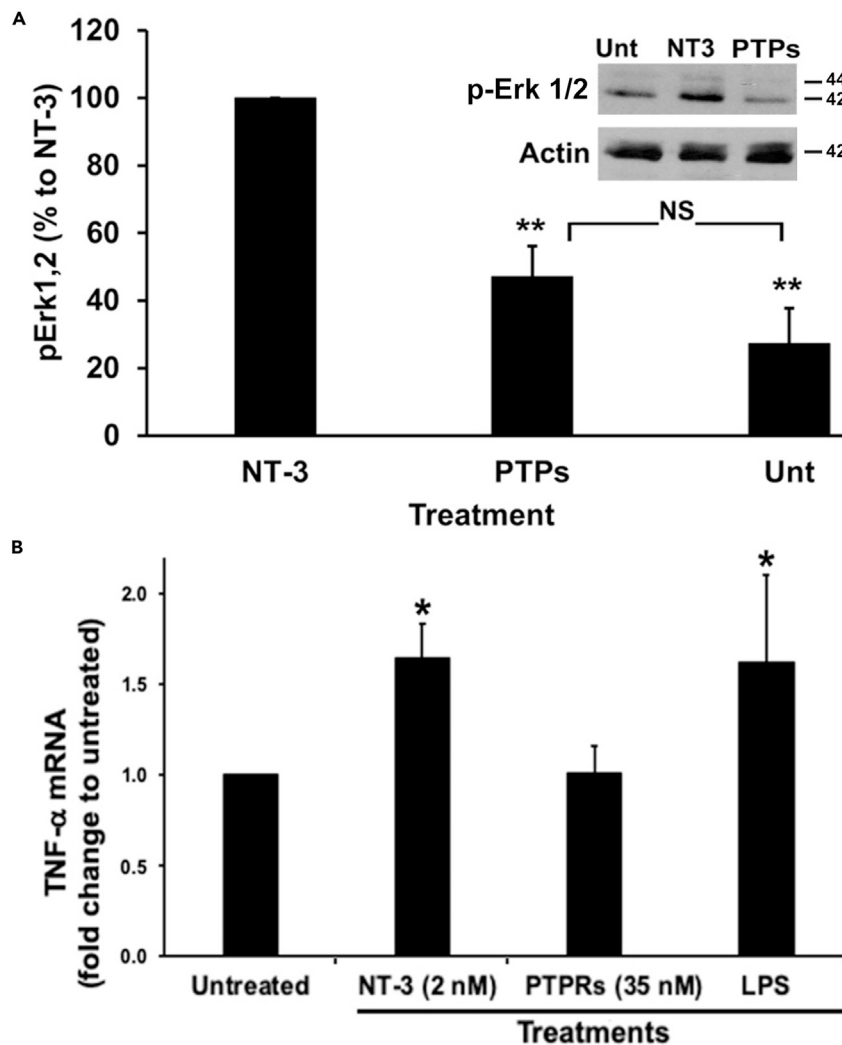


Figure 7. The Ectodomain of PTP-sigma Does Not Activate Key Functions of TrkC.T1

PTP-sigma ectodomain binds to all TrkC isoforms (Figure S4) and was evaluated for TrkC.T1-mediated bioactivity in rMC-TrkC.T1 cells (expressing TrkC.T1). Data are standardized to baseline untreated control or NT-3 positive control. Data are mean \pm standard deviation. Symbols indicate significance, two-tailed t test.

(A) PTP-sigma does not induce pErk1,2 above vehicle control, whereas positive control NT-3 does. An example of a blot is shown as inset. Quantification from three independent experiments, ** $p < 0.01$ versus NT-3 control. NS, not significant. (B) PTP-sigma does not induce TNF- α mRNA above vehicle control. Positive control NT-3 induces TNF- α mRNA, and this is prevented by silencing TrkC.T1 expression (Figure S3). Another positive control, LPS (1 μ g/mL), activates TNF- α mRNA production acting via TOLL-like receptors, and the LPS effect is not affected by silencing TrkC.T1 expression (Figure S3). * $p < 0.05$ versus untreated control.

biological endpoints (only survival is promoted). However, others have shown that PTP-sigma promotes synaptic reorganization equally well through either isoform, but this endpoint is independent of any TrkC-intracellular domain and has no known TrkC-intracellular signals (Coles et al., 2014; Takahashi et al., 2011).

Together, the data indicate that the isoform ectodomain conformations are present *in vivo* (Figure S1), that the isoforms are physiologically relevant, and that the endogenous ligands NT-3 and PTP-sigma do not activate equally and functionally discriminate between isoforms. These concepts are further supported by the discovery of artificial ligands whose binding and function also discriminate between isoforms.

A summary of binding data is shown in Table 1, and a summary of biological data is shown in Table 2. For all ligands, dose-response curves of bioactivity were evaluated, and the effective concentrations (EC) were

	Ligand	TrkC-FL Activity		TrkC.T1 Activity
		Survival	Different	TNF- α mRNA
Not Isoform Selective				
1	NT-3	100	100	100
2	2F5 mAb	22	N.S.	172
3	3G5 mAb	N.S.	N.S.	N.S.
4	1Aa	*71	78	64
Selective TrkC-FL				
5	2B7 mAb	95	N.S.	N.S.
6	3Aa	*65	82	N.S.
7	PTP-sigma	105	N.S.	N.S.
Selective TrkC.T1				
8	1E11 mAb	N.S.	N.S.	236
9	2G5 mAb	N.S.	N.S.	N.S.

Table 2. Functional Efficacy of TrkC Ligands Binding at the Ectodomain

Cell survival and differentiation are the endpoints for TrkC-FL agonism. The endpoints for TrkC.T1 agonism are pErk activation and promotion of TNF- α mRNA and protein. Efficacy and potency are relative to 2 nM NT-3 (set to 100%). All ligands exhibit a dose-dependent pharmacological effect (e.g., [Figures 6A](#) and [S5](#)). The *in vitro* effective concentrations (EC) for each ligand, depending on the assay, are at 0.5–2 nM for NT-3, 20–40 nM for mAbs and PTP-sigma, and 10–50 μ M for small molecules.

NT-3 agonizes all isoforms. PTP-sigma is a biased agonist of TrkC-FL and promotes cell survival but not cell differentiation. PTP-sigma binds to TrkC.T1 but does not activate the TrkC.T1 endpoints studied here. However, PTP-sigma activates the endpoint of synaptic reorganization via TrkC in a non-isoform selective manner and independent of known TrkC signals ([Coles et al., 2014](#); [Takahashi et al., 2011](#)). MAb 2F5 activates both TrkC isoforms (TrkC.T1 with better efficacy than TrkC-FL). MAb 1E11 selectively activates TrkC.T1. MAb 2B7 selectively activates TrkC-FL as a biased agonist, promoting survival but not differentiation (this paper and [Guillemard et al., 2010](#)). MAb 2G5 and 3G5 are non-functional. Small molecules 3Aa and 1Aa promote cell survival with low efficacy, and in survival assays they have high efficacy in combination with 0.1 nM NT-3 (*) above each single treatment (this paper and [Zaccaro et al., 2005](#)). As single treatment, small molecules 3Aa and 1Aa are very efficient at inducing cellular differentiation. 3Aa does not activate TrkC.T1, but 1Aa does. Numbers shown are significant ($p \leq 0.05$), N.S. means not-significant versus controls; two-tailed t test.

determined. In the manuscript, for simplicity we mainly show the optimal ECs, which correspond to approximately 2 nM NT-3, 40 nM for mAbs and PTP-sigma, and 10 μ M for small molecules. MAb 2B7 and PTP-sigma have a maximal efficacy that is comparable with that of NT-3, but they have lower potency (EC₅₀ 2 nM for 2B7 and 8 nM for PTP-sigma, versus EC₅₀ 0.2 nM for NT-3). MAb 2F5 has lower efficacy and potency. Small molecules 3Aa and 1Aa have significantly lower potency and low efficacy. However, 3Aa and 1Aa increase the efficacy of 0.1 nM NT-3, from 25% to 65% and 71%, respectively ([Figure S5](#)).

The different ectodomain structures of TrkC-FL and TrkC.T1 made it possible to discover isoform-selective ligands (mAbs, small molecules, and PTP-sigma) that act as agonists, partial agonists, or biased agonists. The ability of these endogenous or artificial ligands to discriminate binding and/or function takes place despite identical primary ectodomain sequence in TrkC and despite the fact that NT-3 does not discriminate between the naturally occurring receptor isoforms.

DISCUSSION

We report that changes in the intracellular domain primary sequence of a receptor can lead to changes in the ectodomain secondary structure. This finding supports the concept of a bidirectional regulation of receptor conformation: an “outside-to-inside” influence, and an “inside-to-outside” influence. This mechanism increases the known means by which a single gene can generate receptor heterogeneity and signal heterogeneity. We also report on the development of biologically active isoform-selective ligands, even though the primary amino acid sequence of the isoforms is the same and they all bind the natural ligand NT-3.

Out-To-In versus In-To-Out Control of Receptor Conformation

The outside-to-inside conformational influence has been well studied. Ligand binding at the ectodomain of a receptor can cause conformational changes in the transmembrane or the intracellular domains that are required for protein-protein interaction and activation of signaling (Changeux and Christopoulos, 2016; Dawson et al., 2005; Edelstein and Changeux, 2016; Lemmon et al., 2014). The outside-to-inside effect is promoted by ligand binding, can be orthosteric or allosteric, and may be mirrored by receptor over-expression or by receptor mutations inducing or stabilizing an activated transition state in the receptor.

These structural changes have to permeate the lipid bilayer to be reflected in the intracellular domain. The process is highly regulated by the presence of co-receptors and accessory proteins on the same cell surface (homotypic, acting in *cis*-form) or present in the extracellular matrix or in adjoining cell surfaces (heterotypic, acting in *trans*-form), including matrix proteins, lipids and glycolipids, regulators of membrane fluidity, post-translational modifications, and many other factors (Bubliil and Yarden, 2007).

In contrast, the inside-to-outside conformational influence has been less studied. For example, in epidermal growth factor receptors (EGFR) oncogenic mutations or intracellular binding of tyrosine kinase inhibitors can result in altered EGF binding affinity (Macdonald-Obermann and Pike, 2018), potentially through changes in the aggregated state of the receptors or in the ectodomain conformation. Other examples include agents that distinguish between targets that have single amino acid changes, “smart drugs” such as selective c-Src or c-Abl inhibitors (Shawver et al., 2002), or conformationally sensitive mAbs that bind to G-coupled receptors (Heimann et al., 2017) or EGFR family members (Lee et al., 2015), or mAbs and ligands that bind preferentially to homodimers or oligomers (Lemmon and Schlesinger, 2010; Lemmon et al., 2014) or heterodimers (Sweeney et al., 2000). These reports differ from our work because in those cases the receptors have an oncogenic mutation, are pre-activated or over-expressed, or bear the impact of allosteric mechanisms driven by receptor aggregation or by associated co-receptors.

The inside-to-outside effect we report here is independent of ligand binding, independent of changes in primary amino acid sequence or oncogenic transformation, and independent of overexpression or activation. Rather, the effect is caused by alternative splicing of intracellular domains, a process that occurs naturally and is relevant to disease states. Indeed, the alternative splicing of TrkC mRNA impacts in the physiology of many tissues and is implicated in disease onset and disease progression (Bai et al., 2010; Brahimji et al., 2016; Dorsey et al., 2006; Galan et al., 2017; Yanpallewar et al., 2012), highlighting the biological relevance.

Mechanism of the In-To-Out Control of Ectodomain Conformation

The mechanism of inside-to-outside conformational regulation we report implicates receptor association with PDI in the ER, leading to reorganization of disulfide bridges. The conformations of TrkC-FL (and TrkC- Δ -ICD) differ from that of TrkC.T1. TrkC.T1 has disulfides that are formed differently, as determined in proteolytic mapping studies.

The ER is an oxidizing environment and disulfide bonds initially form spontaneously, but often the first bonds to form are not the correct pair, and spontaneous bonding may not form all of the disulfide bonds required. Breaking and re-forming disulfide bonds in the correct combinations is then one rate-limiting step for folding. PDI accelerates rearrangement of the disulfides so the protein can advance from higher free energy intermediates to the final state, which has the lowest free energy (Braakman and Hebert, 2013; Wallis and Freedman, 2013).

Our data support the notion that the native state of the TrkC-FL isoform (and TrkC- Δ -ICD) is a kinetically trapped folding intermediate that has little contribution by PDI. This conformation is different from the TrkC.T1 native state, an isoform where PDI can break and re-form disulfides more efficiently, to reach the final native state. Hence, the energy barrier between TrkC-FL and TrkC.T1 prevents TrkC-FL from adopting the TrkC.T1 native state.

It is noteworthy that, although the main paradigm studied here is a PDI-mediated impact on the structure of TrkC ectodomains, other differences may arise from differential ER/Golgi transit time, such as differential glycosylation. The potentially confounding interference of other post-translational modifications are,

however, excluded in controls in which mild reduction of the TrkC.T1 disulfide bonds generates the TrkC-FL intermediate structure (at least as far as mAb binding is concerned).

Association of PDI with proteins transiting the ER is not unique to TrkC, and the impact of its thiol reductase and isomerase activity have been reported for Integrins, ADAM17 metalloprotease, and thyroid hormone receptors, where PDI association causes changes in their function (Campos et al., 2018; Cho et al., 2012; Lahav et al., 2000). However, to our knowledge a differential impact of PDI on an isoform ectodomain structure has never been reported.

Selective Interaction of TrkC Isoforms with Endogenous Ligands

Initially, we explored the concept that artificial ligands (mAbs and small molecules) may discriminate between the TrkC-FL and TrkC.T1 isoforms. Having succeeded, we then asked whether natural ligands exist that also do this. Two lines of thought prompted this hypothesis. First, the isoforms are naturally occurring and the mAbs recognize the different isoform conformations *in vivo*. Second, if isoforms do not have functionally selective and biased endogenous natural ligands we would be left with the apparent paradox of simultaneous activation of beneficial and toxic pathways by a single ligand, NT-3.

NT-3 is a native growth factor that binds to TrkC and does not discriminate functionally between the isoforms. Another ligand is PTP-sigma, which associates in a heterotypic fashion (on the membrane of a neighboring cell). PTP-sigma binds to TrkC-FL, TrkC.T1, or TrkC- Δ -ICD and can induce synaptic reorganization by causing clustering any of the TrkC isoforms at the synapse, in an NT-3-independent and in a TrkC intracellular domain-independent manner (Coles et al., 2014; Takahashi et al., 2011).

However, functionally PTP-sigma can activate TrkC-FL to promote cell survival signals but without promoting neurotogenic signals or TrkC.T1-mediated promotion of TNF- α production. This is an example of an endogenous TrkC ligand that is a biased agonist, and selectively activates only one of the activities measured, and only in one isoform.

Considering that several splice and glycosylation isoforms of cell surface PTP-sigma are known (Pulido et al., 1995) there may be a high number of permutations of TrkC-PTP-sigma heterotypic interactions. Moreover, we speculate that there may be other TrkC interactors or accessory proteins, homotypic and heterotypic, that could regulate or discriminate between TrkC isoforms in terms of binding or function. These include, for example, p75^{NTR} (Ivanisevic et al., 2003; Maliartchouk and Saragovi, 1997; Zaccaro et al., 2001), which can regulate synaptogenesis (Hapner et al., 1998), ARMS (Zampieri and Chao, 2006), sortilin (Vaegter et al., 2011), or G-coupled receptors (Lee and Chao, 2001; Zampieri and Chao, 2006).

Conformational heterogeneity in isoforms, and a corresponding heterogeneity in their ligands and their interactions, may be an evolutionary strategy that is able to generate numerous combinations or permutations from a small number of gene products, to regulate a high set of biological processes. Ongoing work beyond the scope of this report is studying the relationship of each TrkC isoform with these other proteins, as well as the relationship of PDI with each of these proteins.

Exploiting Ectodomain Conformation for Development of Pharmacological Ligands

We show that it is possible to produce mAbs and small molecules that bind selectively to the ectodomain of naturally occurring TrkC receptor isoforms to differentially activate each isoform. This, in spite of the receptors having identical ectodomain primary amino acid sequences.

These results show that it is possible to differentially target receptor isoforms that play different roles in disease states, to specifically modulate their activity. This is relevant from a translational medicine viewpoint. The artificial agonists reported here could provide better alternatives than NT-3 for treatment of pathologies by selectively targeting the TrkC-FL to promote cell survival, while avoiding activation of TrkC.T1, which drives TNF- α expression to neurotoxic levels (Bai et al., 2010; Brahimi et al., 2016; Galan et al., 2017). The anti-TrkC.T1 mAbs may be developed further as antagonists or may be used to eliminate TrkC.T1-expressing cells (which produce TNF- α) at the onset of degenerative diseases such as glaucoma, retinitis pigmentosa, and ALS (Saragovi et al., 2019) (e.g., Müller glial cells in the retina or activated glia in spinal cord).

Control of Ectodomain Conformation in Receptors

The concept of in-to-out control of receptor conformation may be extended to understanding the many receptors that are alternatively spliced, whether wild-type or oncogenic mutant forms. For example, regarding isoforms in other Trk-family receptors, TrkB has TrkB.T1 and TrkB-T-Shc isoforms generated by use of exon 16 or exon 19, respectively, with alternative polyadenylation signals and translational stops. Deletion of TrkB.T1 is beneficial in a mouse model of ALS (Quarta et al., 2018; Yanpallewar et al., 2012) and in a Down's syndrome mouse model (Dorsey et al., 2006). TrkA has ectodomain isoforms, one of which is relevant to the human disease anhidrosis (Miura et al., 2000), and implicated in responses to noxious stimuli, as well as neuropathic pain (Hefti et al., 2006). Expression of the TrkAIII isoform and other isoforms are correlated with aggressiveness in some type of tumors (Gimm et al., 2001; Tacconelli et al., 2005). All these may be potentially targeted by exploiting conformational differences that may exist in the family.

On the Physiological Role of Receptor Isoforms and Their Ligands

Initially, we explored the concept that artificial ligands (mAbs and small molecules) may discriminate between the TrkC-FL and TrkC.T1 isoforms. Having succeeded, we then asked whether also isoform selective natural ligands exist, given that the receptors are naturally occurring. Otherwise we would be left with the apparent paradox of simultaneous activation of beneficial and toxic pathways by NT-3. The ligand PTP-sigma was an obvious choice, as its role in TrkC-mediated synaptic reorganization was published to be promoted through either isoform, and it is independent of a TrkC intracellular domain or any known direct signal transduction (Coles et al., 2014; Takahashi et al., 2011) and no isoform differences were reported for that specific endpoint. However, to our surprise no other endpoints had been reported for PTP-sigma acting via TrkC (i.e., no cell survival or neuronal differentiation were reported).

In our studies using additional endpoints we find that PTP-sigma can discriminate functionally between TrkC isoforms, even though it binds to all isoforms. PTP-sigma activates TrkC-FL as a biased agonist, with distinct kinetics that promote cell survival signals but without activating neurotogenic signals. Moreover PTP-sigma does not activate the endpoint of TrkC.T1-mediated promotion of TNF- α to neurotoxic levels (Brahimi et al., 2016; Galan et al., 2017).

Regarding a role for TrkC-FL and TrkC.T1, neuronal development is one case where each isoform and their ligands may play unique roles. This heterogeneity in receptors and ligands may be a mechanism for modulating signals in TrkC populations, acting as a rheostat to bias signals (e.g., to survival or differentiation) or to regulate or stabilize synapses that arise *de novo* during the process of neuronal plasticity.

Although both TrkC-FL and TrkC.T1 receptors are expressed during CNS development (Menn et al., 1998), they differ in spatiotemporal and cellular compartmentalization (Menn et al., 2000). The distinct intracellular signaling pathways (phospholipase C, Ras, PI3 for TrkC-FL; tamalin-Arfs and Rac1 GTPases for TrkC.T1) might explain the different roles in synaptic development and maturation (Rizzo et al., 2018) (Kronschlager et al., 2016) (Oshima et al., 2009).

For example, TNF- α mediates synaptic loss (Henstridge et al., 2019) and in disease (depending on the levels) can contribute to functional changes in synaptic plasticity in a deleterious (Kronschlager et al., 2016; Rizzo et al., 2018) or protective manner (Oshima et al., 2009). Hence, PTP-sigma•TrkC.T1 promotion of TNF- α could balance NT-3•TrkC-FL signals. Indeed, neurons expressing TrkC-FL showed enhancement of major axonal processes, whereas the truncated isoform reduced elongation of major processes but increased their branching (Ichinose and Snider, 2000). This, in part, may also be dependent on co-expression of p75 co-receptors (Hapner et al., 1998). It is also noteworthy that, unrelated to TrkC activity, PTP-sigma also regulates axonal growth after injury and inhibits axon regeneration (Sapieha et al., 2005; Thompson et al., 2003).

Conclusions

The development of mAb and small molecule artificial ligands that discriminate TrkC isoforms, as well as the finding of an endogenous ligand PTP-sigma that discriminates TrkC isoforms, enabled binding and functional assays that support the notion of conformational differences at the ectodomain. Conformational differences are supported also by protein mapping and biochemical characterization of the disulfide binding patterns and association with PDI.

Conformational characterization is not feasible using techniques for structural studies (e.g., crystallography or NMR on soluble receptor isoforms) because the absence of intracellular domain yields a single ectodomain conformation, e.g., TrkC- Δ -ICD is identical to TrkC-FL as far as recognition by all the ligands and the interaction with PDI is concerned. In that regard, our results yield a cautionary note with respect to the structure of the ectodomains of cell surface receptors that are engineered at their intracellular domains or that are engineered to be secreted as soluble proteins. The engineering could lead to alternate ectodomain conformation or to disulfide bonding that is entropically driven (Braakman and Hebert, 2013; Kozlov et al., 2010b; Wallis and Freedman, 2013) and may lose any kinetically driven conformations or disulfide bonding. The conformation of such engineered receptors may not correspond to the conformation on the cell membrane, yet the proteins could still be able to bind to ligands and mAbs. CryoEM techniques or the TM cleavage followed by purification of receptor isoforms after cell surface expression may be possible approaches to extend this study.

This paper validates the concept that naturally occurring variants of a receptor intracellular domain can impact on the conformation of the ectodomain (in-to-out effect) to enable isoform-selective ligands with biased bioactivity, both naturally occurring ligands (PTP-sigma) or artificial ligands (mAbs or small molecules). This strategy may be applied to other receptors.

Limitations of the Study

- 1 Structural studies using soluble TrkC.T1 isoform ectodomain are not feasible. The absence of an intracellular domain (as we demonstrate for TrkC- Δ -ICD) yields an ectodomain conformation that folds like the TrkC-FL.
- 2 Purification of the ectodomain of receptor isoforms cleaved from the cell surface may be a suitable approach but was not attempted. Perhaps cryo-EM on membrane proteins might be useful, but the resolution is unlikely to be adequate.
- 3 The presence of different ectodomain protein structures for TrkC-FL and TrkC.T1 (recognized by the different mAbs) was shown *in vivo* to change in disease, but most of the conclusions regarding signaling pathways are based on the use of cell lines.
- 4 Biochemical characterization of the isoforms and their association with PDI is based on the use of cell lines.
- 5 The precise pairs of disulfide-bonded cysteines were not identified in TrkC.T1.
- 6 Receptor isoform internalization and recycling, and glycosylation, were not evaluated.

Resource Availability

Lead Contact

Further information and request for resources and reagents should be directed to and will be fulfilled by the Lead Contact, Dr. H. Uri Saragovi (uri.saragovi@mcgill.ca).

Materials Availability

Reagents generated in this study will be made available on request, but we may require a payment of costs and/or a completed Materials Transfer Agreement.

Data and Code Availability

This study did not generate/analyze datasets or code. Original data for figures and tables in the paper are available from the corresponding author on request.

METHODS

All methods can be found in the accompanying [Transparent Methods supplemental file](#).

SUPPLEMENTAL INFORMATION

Supplemental Information can be found online at <https://doi.org/10.1016/j.isci.2020.101447>.

ACKNOWLEDGMENTS

We thank Dr. Hinyu Nedev (Lady Davis Institute) for peptide synthesis and Anne Marcil (National Research Council Canada) for expert assistance with hybridoma fusions. This work was funded by grants to H.U.S. from the Canadian Institutes of Health Research (Pharmacology) and the Canadian Consortium on Neurodegeneration in Aging (CCNA).

AUTHOR CONTRIBUTIONS

Conceptualization, F.B., J.C.Y., D.Y.T., and H.U.S. Methodology, F.B., A.G., N.D.J., K.D., C.K., D.Y.T., and H.U.S. Formal Analysis, F.B., A.G., S.J., N.D.J., K.D., J.C.Y., C.K., D.Y.T., and H.U.S. Investigation, F.B., A.G., S.J., P.F.B., N.D.J., and K.D. Data Curation, A.G., C.K., and H.U.S. Writing – Original Draft, Writing – Review & Editing, J.C.Y., C.K., D.Y.T., and H.U.S. Supervision, C.K., D.Y.T., and H.U.S. Project Administration and Funding Acquisition, H.U.S.

DECLARATION OF INTERESTS

Authors have patent holdings and applications for ligands and bioactivities that are related to the subject matter of the contribution (F.B. and H.U.S. inventors).

Received: February 19, 2020

Revised: May 13, 2020

Accepted: August 6, 2020

Published: September 25, 2020

REFERENCES

- Bai, Y., Shi, Z., Zhuo, Y., Liu, J., Malakhov, A., Ko, E., Burgess, K., Schaefer, H., Esteban, P.F., Tessarollo, L., et al. (2010). In glaucoma the upregulated truncated TrkC.T1 receptor isoform in glia causes increased TNF- α production, leading to retinal ganglion cell death. *Invest. Ophthalmol. Vis. Sci.* 51, 6639–6651.
- Braakman, I., and Hebert, D.N. (2013). Protein folding in the endoplasmic reticulum. *Cold Spring Harb Perspect. Biol.* 5, a013201.
- Brahimi, F., Liu, J., Malakhov, A., Chowdhury, S., Purisima, E.O., Ivanisevic, L., Caron, A., Burgess, K., and Saragovi, H.U. (2010). A monovalent agonist of TrkA tyrosine kinase receptors can be converted into a bivalent antagonist. *Biochim. Biophys. Acta* 1800, 1018–1026.
- Brahimi, F., Maira, M., Barcelona, P.F., Galan, A., Aboukassim, T., Teske, K., Rogers, M.L., Bertram, L., Wang, J., Yousefi, M., et al. (2016). The paradoxical signals of two TrkC receptor isoforms supports a rationale for novel therapeutic strategies in ALS. *PLoS One* 11, e0162307.
- Bublil, E.M., and Yarden, Y. (2007). The EGF receptor family: spearheading a merger of signaling and therapeutics. *Curr. Opin. Cell Biol.* 19, 124–134.
- Campos, J.L.O., Doratioto, T.R., Videira, N.B., Ribeiro Filho, H.V., Batista, F.A.H., Fattori, J., Indolfo, N.C., Nakahira, M., Bajgelman, M.C., Cvorovic, A., et al. (2018). Protein disulfide isomerase modulates the activation of thyroid hormone receptors. *Front. Endocrinol. (Lausanne)* 9, 784.
- Changeux, J.P., and Christopoulos, A. (2016). Allosteric modulation as a unifying mechanism for receptor function and regulation. *Cell* 166, 1084–1102.
- Chen, D., Brahimi, F., Angell, Y., Li, Y.C., Moscovitz, J., Saragovi, H.U., and Burgess, K. (2009). Bivalent peptidomimetic ligands of TrkC are biased agonists and selectively induce neurite outgrowth or potentiate neurotrophin-3 trophic signals. *ACS Chem. Biol.* 4, 769–781.
- Cho, J., Kennedy, D.R., Lin, L., Huang, M., Merrill-Skoloff, G., Furie, B.C., and Furie, B. (2012). Protein disulfide isomerase capture during thrombus formation in vivo depends on the presence of beta3 integrins. *Blood* 120, 647–655.
- Coles, C.H., Mitakidis, N., Zhang, P., Elegheert, J., Lu, W., Stoker, A.W., Nakagawa, T., Craig, A.M., Jones, E.Y., and Aricescu, A.R. (2014). Structural basis for extracellular cis and trans RPTsigma signal competition in synaptogenesis. *Nat. Commun.* 5, 5209.
- Dawson, J.P., Berger, M.B., Lin, C.C., Schlessinger, J., Lemmon, M.A., and Ferguson, K.M. (2005). Epidermal growth factor receptor dimerization and activation require ligand-induced conformational changes in the dimer interface. *Mol. Cell Biol.* 25, 7734–7742.
- Deinhardt, K., and Chao, M.V. (2014). Trk receptors. *Handb. Exp. Pharmacol.* 220, 103–119.
- Dorsey, S.G., Renn, C.L., Carim-Todd, L., Barrick, C.A., Bambrick, L., Krueger, B.K., Ward, C.W., and Tessarollo, L. (2006). In vivo restoration of physiological levels of truncated TrkC.T1 receptor rescues neuronal cell death in a trisomic mouse model. *Neuron* 51, 21–28.
- Edelstein, S.J., and Changeux, J.P. (2016). Biased allostery. *Biophys. J.* 111, 902–908.
- Esteban, P.F., Yoon, H.Y., Becker, J., Dorsey, S.G., Caprari, P., Palko, M.E., Coppola, V., Saragovi, H.U., Randazzo, P.A., and Tessarollo, L. (2006). A kinase-deficient TrkC receptor isoform activates Arf6-Rac1 signaling through the scaffold protein tamalin. *J. Cell Biol.* 173, 291–299.
- Galan, A., Jmaeff, S., Barcelona, P.F., Brahimi, F., Sarunic, M.V., and Saragovi, H.U. (2017). In retinitis pigmentosa TrkC.T1-dependent vectorial Erk activity upregulates glial TNF- α , causing selective neuronal death. *Cell Death Dis* 8, 3222.
- Geva, Y., and Schuldiner, M. (2014). The back and forth of cargo exit from the endoplasmic reticulum. *Curr. Biol.* 24, R130–R136.
- Gimm, O., Dziema, H., Brown, J., de la Puente, A., Hoang-Vu, C., Dralle, H., Plass, C., and Eng, C. (2001). Mutation analysis of NTRK2 and NTRK3, encoding 2 tyrosine kinase receptors, in sporadic human medullary thyroid carcinoma reveals novel sequence variants. *Int. J. Cancer* 92, 70–74.
- Guillemard, V., Ivanisevic, L., Garcia, A.G., Scholten, V., Lazo, O.M., Bronfman, F.C., and Saragovi, H.U. (2010). An agonistic mAb directed to the TrkC receptor juxtamembrane region defines a trophic hot spot and interactions with p75 coreceptors. *Dev. Neurobiol.* 70, 150–164.
- Hapner, S.J., Boeshore, K.L., Large, T.H., and Lefcort, F. (1998). Neural differentiation promoted by truncated trkC receptors in collaboration with p75(NTR). *Dev. Biol.* 201, 90–100.
- Hefti, F.F., Rosenthal, A., Walicke, P.A., Wyatt, S., Vergara, G., Shelton, D.L., and Davies, A.M. (2006). Novel class of pain drugs based on antagonism of NGF. *Trends Pharmacol. Sci.* 27, 85–91.
- Heimann, A.S., Gupta, A., Gomes, I., Rayees, R., Schlessinger, A., Ferro, E.S., Unterwald, E.M., and Devi, L.A. (2017). Generation of G protein-coupled receptor antibodies differentially sensitive to conformational states. *PLoS One* 12, e0187306.

- Henstridge, C.M., Hyman, B.T., and Spire-Jones, T.L. (2019). Beyond the neuron-cellular interactions early in Alzheimer disease pathogenesis. *Nat. Rev. Neurosci.* 20, 94–108.
- Ichinose, T., and Snider, W.D. (2000). Differential effects of TrkC isoforms on sensory axon outgrowth. *J. Neurosci. Res.* 59, 365–371.
- Ivanisevic, L., Banerjee, K., and Saragovi, H.U. (2003). Differential cross-regulation of TrkA and TrkC tyrosine kinase receptors with p75. *Oncogene* 22, 5677–5685.
- Kozlov, G., Azeroual, S., Rosenauer, A., Maattanen, P., Denisov, A.Y., Thomas, D.Y., and Gehring, K. (2010a). Structure of the catalytic $\alpha(0)$ fragment of the protein disulfide isomerase ERp72. *J. Mol. Biol.* 401, 618–625.
- Kozlov, G., Maattanen, P., Thomas, D.Y., and Gehring, K. (2010b). A structural overview of the PDI family of proteins. *FEBS J.* 277, 3924–3936.
- Kronschlager, M.T., Drdla-Schutting, R., Gassner, M., Honsek, S.D., Teuchmann, H.L., and Sandkuhler, J. (2016). Gliogenic LTP spreads widely in nociceptive pathways. *Science* 354, 1144–1148.
- Lahav, J., Gofer-Dadosh, N., Luboshitz, J., Hess, O., and Shaklai, M. (2000). Protein disulfide isomerase mediates integrin-dependent adhesion. *FEBS Lett.* 475, 89–92.
- Lee, F., and Chao, M. (2001). Activation of Trk neurotrophin receptors in the absence of neurotrophins. *Proc. Natl. Acad. Sci. U S A* 98, 3555–3560.
- Lee, R.J., Liu, C.W., Harty, C., McCracken, A.A., Latterich, M., Romisch, K., DeMartino, G.N., Thomas, P.J., and Brodsky, J.L. (2004). Uncoupling retro-translocation and degradation in the ER-associated degradation of a soluble protein. *EMBO J.* 23, 2206–2215.
- Lee, S., Greenlee, E.B., Amick, J.R., Ligon, G.F., Lillquist, J.S., Natoli, E.J., Jr., Hadari, Y., Alvarado, D., and Schlessinger, J. (2015). Inhibition of ErbB3 by a monoclonal antibody that locks the extracellular domain in an inactive configuration. *Proc. Natl. Acad. Sci. U S A* 112, 13225–13230.
- Lemmon, M.A., and Schlessinger, J. (2010). Cell signaling by receptor tyrosine kinases. *Cell* 141, 1117–1134.
- Lemmon, M.A., Schlessinger, J., and Ferguson, K.M. (2014). The EGFR family: not so prototypical receptor tyrosine kinases. *Cold Spring Harb. Perspect. Biol.* 6, a020768.
- Macdonald-Obermann, J.L., and Pike, L.J. (2018). Allosteric regulation of epidermal growth factor (EGF) receptor ligand binding by tyrosine kinase inhibitors. *J. Biol. Chem.* 293, 13401–13414.
- Maliartchouk, S., and Saragovi, H.U. (1997). Optimal nerve growth factor trophic signals mediated by synergy of TrkA and p75 receptor-specific ligands. *J. Neurosci.* 17, 6031–6037.
- Matsusaki, M., Kanemura, S., Kinoshita, M., Lee, Y.H., Inaba, K., and Okumura, M. (2020). The protein disulfide isomerase family: from proteostasis to pathogenesis. *Biochim. Biophys. Acta Gen. Subj.* 1864, 129338.
- Menn, B., Timsit, S., Calothy, G., and Lamballe, F. (1998). Differential expression of TrkC catalytic and noncatalytic isoforms suggests that they act independently or in association. *J. Comp. Neurol.* 401, 47–64.
- Menn, B., Timsit, S., Represa, A., Mateos, S., Calothy, G., and Lamballe, F. (2000). Spatiotemporal expression of noncatalytic TrkC NC2 isoform during early and late CNS neurogenesis: a comparative study with TrkC catalytic and p75NTR receptors. *Eur. J. Neurosci.* 12, 3211–3223.
- Michelsen, K., Yuan, H., and Schwappach, B. (2005). Hide and run. Arginine-based endoplasmic-reticulum-sorting motifs in the assembly of heteromultimeric membrane proteins. *EMBO Rep.* 6, 717–722.
- Miura, Y., Mardy, S., Awaya, Y., Nihei, K., Endo, F., Matsuda, I., and Indo, Y. (2000). Mutation and polymorphism analysis of the TRKA (NTRK1) gene encoding a high-affinity receptor for nerve growth factor in congenital insensitivity to pain with anhidrosis (CIPA) families. *Hum. Genet.* 106, 116–124.
- Oshima, T., Lee, S., Sato, A., Oda, S., Hirasawa, H., and Yamashita, T. (2009). TNF- α contributes to axonal sprouting and functional recovery following traumatic brain injury. *Brain Res.* 1290, 102–110.
- Palko, M.E., Coppola, V., and Tessarollo, L. (1999). Evidence for a role of truncated trkC receptor isoforms in mouse development. *J. Neurosci.* 19, 775–782.
- Pulido, R., Serra-Pages, C., Tang, M., and Streuli, M. (1995). The LAR/PTP delta/PTP sigma subfamily of transmembrane protein-tyrosine-phosphatases: multiple human LAR, PTP delta, and PTP sigma isoforms are expressed in a tissue-specific manner and associate with the LAR-interacting protein LIP-1. *Proc. Natl. Acad. Sci. U S A* 92, 11686–11690.
- Quarta, E., Fulgenzi, G., Bravi, R., Cohen, E.J., Yanpallewar, S., Tessarollo, L., and Minciaccchi, D. (2018). Deletion of the endogenous TrkB.T1 receptor isoform restores the number of hippocampal CA1 parvalbumin-positive neurons and rescues long-term potentiation in pre-symptomatic mSOD1(G93A) ALS mice. *Mol. Cell Neurosci.* 89, 33–41.
- Rizzo, F.R., Musella, A., De Vito, F., Fresegna, D., Bullitta, S., Vanni, V., Guadalupi, L., Stampanoni Bassi, M., Buttari, F., Mandolesi, G., et al. (2018). Tumor necrosis factor and interleukin-1 β modulate synaptic plasticity during neuroinflammation. *Neural Plast.* 2018, 8430123.
- Sapieha, P.S., Duplan, L., Uetani, N., Joly, S., Tremblay, M.L., Kennedy, T.E., and Di Polo, A. (2005). Receptor protein tyrosine phosphatase sigma inhibits axon regrowth in the adult injured CNS. *Mol. Cell Neurosci.* 28, 625–635.
- Saragovi, H.U., Galan, A., and Levin, L.A. (2019). Neuroprotection: pro-survival and anti-neurotoxic mechanisms as therapeutic strategies in neurodegeneration. *Front. Cell Neurosci.* 13, 231.
- Saragovi, H.U., Hamel, E., and Di Polo, A. (2009). A neurotrophic rationale for the therapy of neurodegenerative disorders. *Curr. Alzheimer Res.* 6, 419–423.
- Saragovi, H.U., Zheng, W., Maliartchouk, S., DiGuglielmo, G.M., Mawal, Y.R., Kamen, A., Woo, S.B., Cuello, A.C., Debeir, T., and Neet, K.E. (1998). A TrkA-selective, fast internalizing nerve growth factor-antibody complex induces trophic but not neurotogenic signals. *J. Biol. Chem.* 273, 34933–34940.
- Segal, R.A. (2003). Selectivity in neurotrophin signaling: theme and variations. *Annu. Rev. Neurosci.* 26, 299–330.
- Sendtner, M., Holtmann, B., and Hughes, R.A. (1996). The response of motoneurons to neurotrophins. *Neurochem. Res.* 21, 831–841.
- Shawver, L.K., Slamon, D., and Ullrich, A. (2002). Smart drugs: tyrosine kinase inhibitors in cancer therapy. *Cancer Cell* 1, 117–123.
- Sweeney, C., Lai, C., Riese, D.J., 2nd, Diamonti, A.J., Cantley, L.C., and Carraway, K.L., 3rd (2000). Ligand discrimination in signaling through an ErbB4 receptor homodimer. *J. Biol. Chem.* 275, 19803–19807.
- Szobota, S., Mathur, P.D., Siegel, S., Black, K., Saragovi, H.U., and Foster, A.C. (2019). BDNF, NT-3 and Trk receptor agonist monoclonal antibodies promote neuron survival, neurite extension, and synapse restoration in rat cochlea ex vivo models relevant for hidden hearing loss. *PLoS One* 14, e0224022.
- Tacconelli, A., Farina, A.R., Cappabianca, L., Gulino, A., and Mackay, A.R. (2005). Alternative TrkAIII splicing: a potential regulated tumor-promoting switch and therapeutic target in neuroblastoma. *Future Oncol.* 1, 689–698.
- Takahashi, H., Arstikaitis, P., Prasad, T., Bartlett, T.E., Wang, Y.T., Murphy, T.H., and Craig, A.M. (2011). Postsynaptic TrkC and presynaptic PTPsigma function as a bidirectional synaptic organizing complex. *Neuron* 69, 287–303.
- Tessarollo, L., Tsoulfas, P., Donovan, M.J., Palko, M.E., Blair-Flynn, J., Hempstead, B.L., and Parada, L.F. (1997). Targeted deletion of all isoforms of the trkC gene suggests the use of alternate receptors by its ligand neurotrophin-3 in neuronal development and implicates trkC in normal cardiogenesis. *Proc. Natl. Acad. Sci. U S A* 94, 14776–14781.
- Thompson, K.M., Uetani, N., Manitt, C., Elchebly, M., Tremblay, M.L., and Kennedy, T.E. (2003). Receptor protein tyrosine phosphatase sigma inhibits axonal regeneration and the rate of axon extension. *Mol. Cell Neurosci.* 23, 681–692.
- Tsoulfas, P., Soppet, D., Escandon, E., Tessarollo, L., Mendoza-Ramirez, J.L., Rosenthal, A., Nikolics, K., and Parada, L.F. (1993). The rat trkC locus encodes multiple neurogenic receptors that exhibit differential response to neurotrophin-3 in PC12 cells. *Neuron* 10, 975–990.
- Urfer, R., Tsoulfas, P., O'Connell, L., Hongo, J.-A., Zhao, W., and Presta, L.G. (1998). High resolution mapping of the binding site of TrkA for nerve growth factor and TrkC for neurotrophin-3 on the second immunoglobulin-like domain of the Trk receptors. *J. Biol. Chem.* 273, 5829–5840.

Urfer, R., Tsoulfas, P., O'Connell, L., Shelton, D., Parada, L., and Presta, L. (1995). An immunoglobulin-like domain determines the specificity of neurotrophin receptors. *EMBO J.* 14, 2795–2805.

Vaegter, C.B., Jansen, P., Fjorback, A.W., Glerup, S., Skeldal, S., Kjolby, M., Richner, M., Erdmann, B., Nyengaard, J.R., Tessarollo, L., et al. (2011). Sortilin associates with Trk receptors to enhance anterograde transport and neurotrophin signaling. *Nat. Neurosci.* 14, 54–61.

Wallis, A.K., and Freedman, R.B. (2013). Assisting oxidative protein folding: how do protein disulphide-isomerases couple conformational and chemical processes in protein folding? *Top. Curr. Chem.* 328, 1–34.

Yanpallewar, S.U., Barrick, C.A., Buckley, H., Becker, J., and Tessarollo, L. (2012). Deletion of the BDNF truncated receptor TrkB.T1 delays disease onset in a mouse model of amyotrophic lateral sclerosis. *PLoS One* 7, e39946.

Youn, Y.H., Feng, J., Tessarollo, L., Ito, K., and Sieber-Blum, M. (2003). Neural crest stem cell and cardiac endothelium defects in the TrkC null mouse. *Mol. Cell Neurosci.* 24, 160–170.

Zaccaro, M.C., Ivanisevic, L., Perez, P., Meakin, S.O., and Saragovi, H.U. (2001). p75 Co-receptors regulate ligand-dependent and ligand-independent Trk receptor activation, in part by altering Trk docking subdomains. *J. Biol. Chem.* 276, 31023–31029.

Zaccaro, M.C., Lee, H.B., Pattarawarapan, M., Xia, Z., Caron, A., L'Heureux, P.J., Bengio, Y., Burgess, K., and Saragovi, H.U. (2005). Selective small molecule peptidomimetic ligands of TrkC and TrkA receptors afford discrete or complete neurotrophic activities. *Chem. Biol.* 12, 1015–1028.

Zampieri, N., and Chao, M.V. (2006). Mechanisms of neurotrophin receptor signalling. *Biochem. Soc. Trans.* 34, 607–611.

Zhang, Y., Moheban, D.B., Conway, B.R., Bhattacharyya, A., and Segal, R.A. (2000). Cell surface Trk receptors mediate NGF-induced survival while internalized receptors regulate NGF-induced differentiation. *J. Neurosci.* 20, 5671–5678.

iScience, Volume 23

Supplemental Information

Alternative Splicing of a Receptor Intracellular Domain Yields Different Ectodomain Conformations, Enabling Isoform-Selective Functional Ligands

Fouad Brahim, Alba Galan, Sean Jmaeff, Pablo F. Barcelona, Nicolas De Jay, Kurt Dejpgard, Jason C. Young, Claudia L. Kleinman, David Y. Thomas, and H. Uri Saragovi

SUPPLEMENTAL FIGURES

Figure S1. 1E11 and 1B2 mAbs bind selectively to upregulated TrkC.T1 protein in sections of ALS spinal cord. Related to Figure 1 and Tables 1 and 2. Spinal cord sections of 12 μm were prepared from G93A ALS mice or wild type mice (ventral horn, lumbar region L2-L3). TrkC.T1 protein (red) was identified using selective anti-TrkC.T1 mAb **1E11** (ectodomain) or anti-TrkC.T1 mAb **1B2** (intracellular domain). Glia is localized using the GFAP marker (green). Pictures were taken using a Leica spinning disc confocal microscope with 63x magnification. **A. 1E11** staining. **B. 1B2** staining. **C.** Negative control in the absence of primary antibody. The insets show a higher magnification of the small white rectangles. Scale bar 7 μm . Similar staining data was obtained from thoracic sections (data not shown).

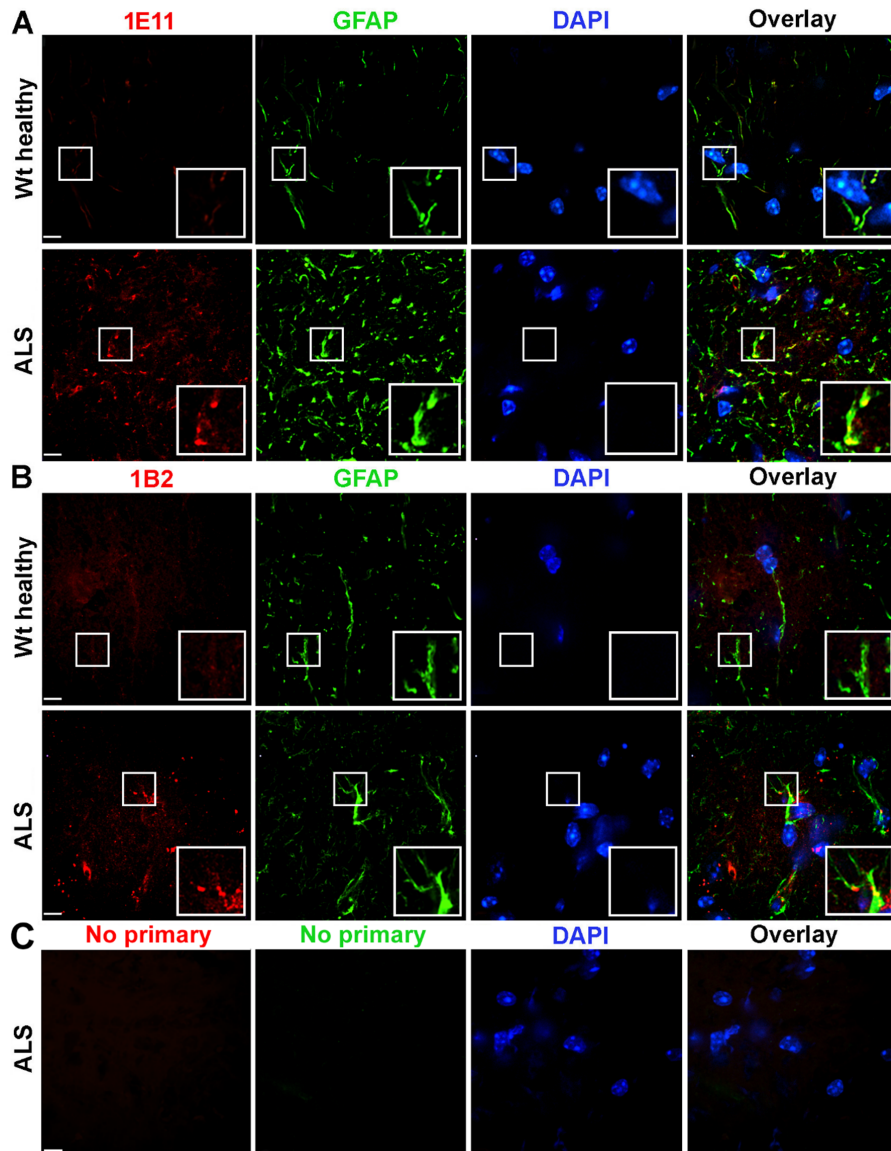


Figure S2. ER retention or export sequences in the intracellular domain of human TrkC isoforms. Related to Figure 2. Underlining indicates the transmembrane domain. Bold indicates the unique spliced-in sequence added to TrkC.T1. Light shading indicates ER exit sequences (7 in TrkC-FL and 4 in TrkC.T1). Dark shading indicates ER retrieval sequences (2 sites in TrkC-FL). TrkC- Δ -ICD does not have an intracellular domain, and has no ER exit or ER retrieval sequences.

hTrkC.T1

FGVSIAVGLAAFACVLLVVLFVMINKYGRRSKFGM
 KGPVAVISGEEDSASPLHHINHGITTPSSLDAGPDTV
 VIGMTRIPVIENPQYFRQGHNCHKPDTWVFSNIDN
HGILNLKDNRDHLVPSTHYIYEPEVQSGEVSYP
RSHGFREIMLNPISLPGH**SKPLNHGIYVEDVNVY**
FSKGRHGF

hTrkC-FL

FGVSIAVGLAAFACVLLVVLFVMINKYGRRSKFGM
 KGPVAVISGEEDSASPLHHINHGITTPSSLDAGPDTV
 VIGMTRIPVIENPQYFRQGHNCHKPDTYVQHIKRRD
 IVLKRELGEAFAFGKVFLAECYNLSPTKDKMLVAVK
 ALKDPTLAARKDFQREAEELLTNLQHEHIVKFYGVC
 GDGDPLIMVF EYMKHGDLNKFLRAHGPDAMILVD
 GQPRQAKGELGLSQMLHIASQIASGMVYLASQHFV
 HRDLATRNLVGANLLVKIGDFGMSRDVYSTDY
 RLFNPSGNDFCIWCEVGGHTMLPIRWPPESIMYR
 KFTTESDVWSFGVILWEIFTYGKQPWFQLSNTEVIE
 CITQGRVLERPRVCPKEVYDVMLGCWQREPQQRL
 NIKEIYKILHALGKATPIYLDILG

Figure S3. MAb 1E11–promoted increase in TNF α mRNA requires TrkC.T1 expression

Related to Figure 4 and Figure 7B. rMC-1 glial cells expressing TrkC.T1 were infected with scrambled control (white bars) or with pLKO-1 virus (black bars) to silence TrkC.T1 expression (Brahimi et al., 2016). After infection the cells were treated with vehicle (untreated control), mAb 1E11, or NT-3 and LPS controls. TNF α mRNA levels were quantified 6 hours after ligand treatment, by quantitative real-time PCR. Compared to untreated control, all the treatments significantly ($p < 0.001$) induced TNF α mRNA in the scrambled virus infected control groups (white bars). Data are mean \pm standard deviation. Symbols indicate significance. Silencing TrkC.T1 reduced the effect of mAb 1E11 or NT-3, indicating that these agonists act in a TrkC.T1–dependent manner. Silencing of TrkC.T1 did not affect LPS–induced TNF α mRNA, as expected because LPS acts via Toll-like receptors. The brackets indicate significant differences in ligand-promoted induction of TNF α mRNA (* $p < 0.05$. ** $p < 0.01$; one-way ANOVA with Tukey-Kramer Multiple comparisons).

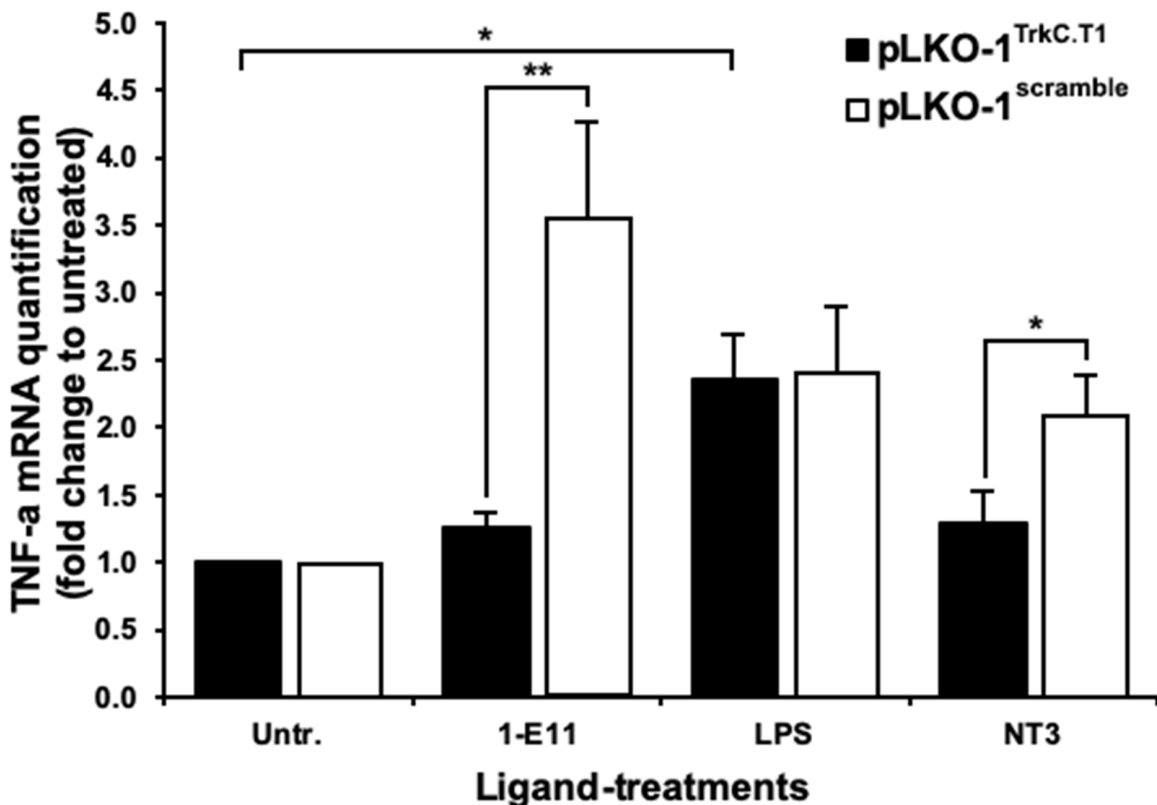


Figure S4. PTP-sigma ectodomain binds to the ectodomain of all TrkC isoforms.

Related to Figures 6 and 7 and Tables 1 and 2. Flow cytometry binding assays using HEK293 cells each stably expressing each isoform. TrkC-FL (black), TrkC.T1 (dashed), or TrkC- Δ -ICD (gray) expressing cells were immunolabeled. **A.** PTP-sigma ectodomain (10 nM). **B.** MAb 2F5 (binding to all isoforms) is a positive control. Irrelevant IgG (red histogram) is a negative control. The same background is seen for all cell types but for simplicity only one background histogram is depicted.

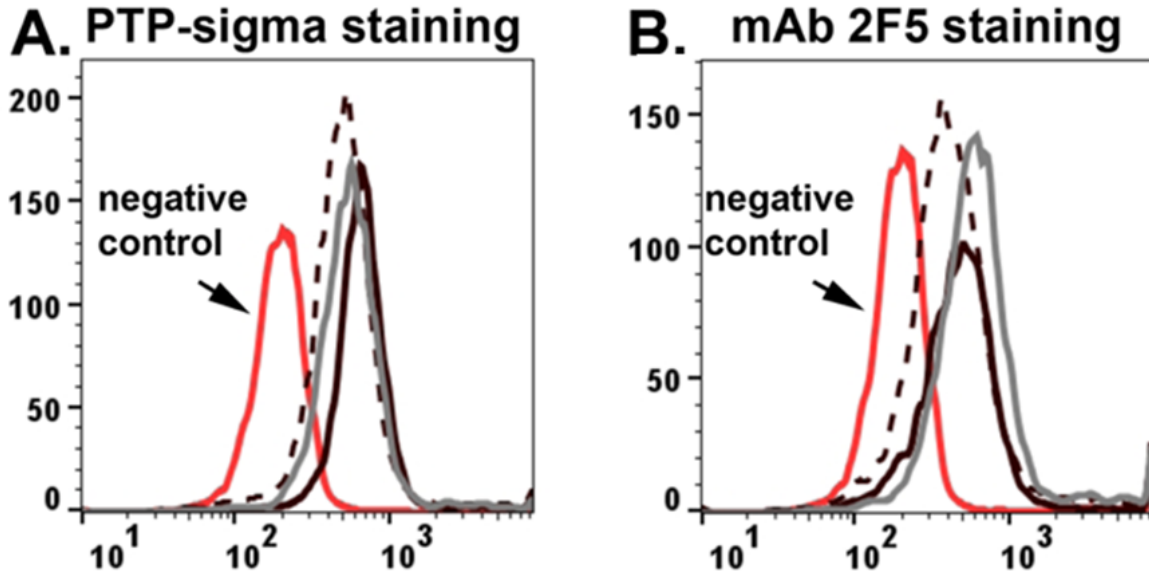
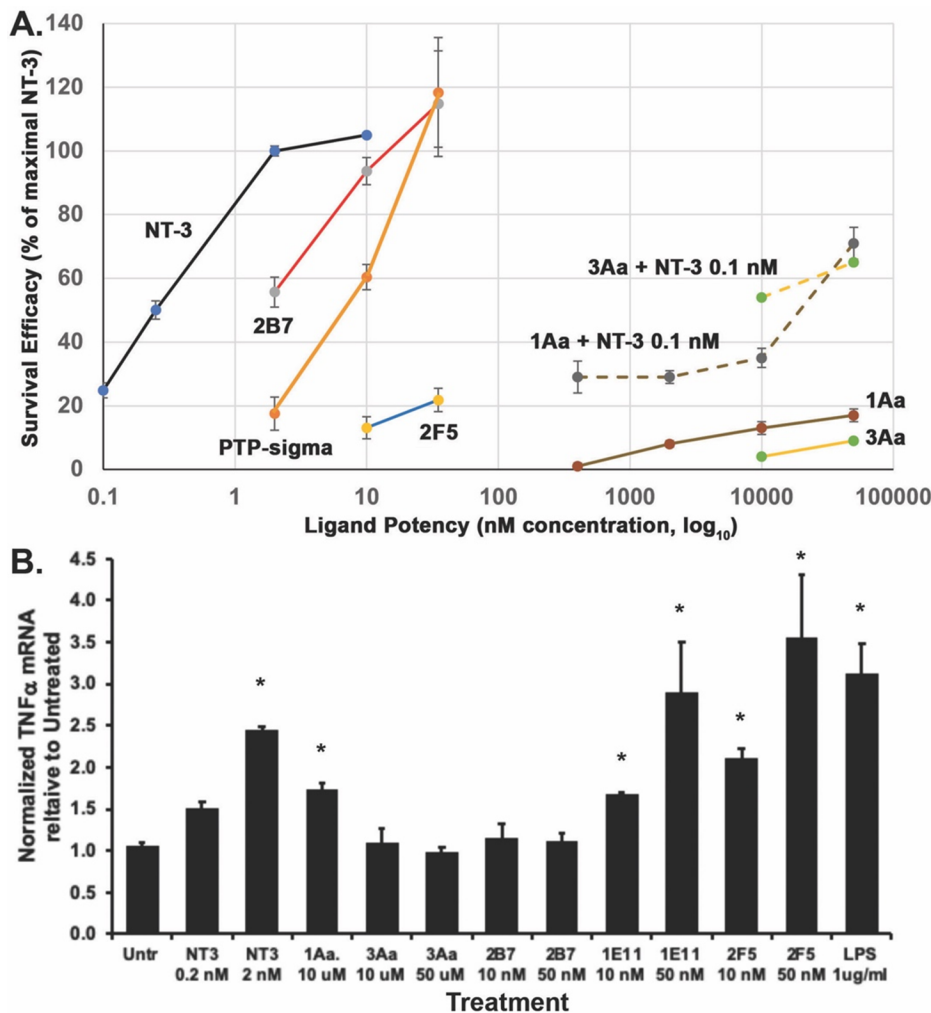


Figure S5. Dose-dependent profiles of TrkC agonists

Related to Figures 4, 5, and 6 and Tables 1 and 2. Dose-response curves of bioactivity were evaluated for all ligands. Shown are the bioactive agents, some inactive ligands are omitted.

A. TrkC-FL agonist promotion of HEK293-TrkC-FL cell survival in serum-free culture conditions. Potency is determined from the effective concentrations (EC). Mab 2B7 and PTP-sigma have a maximal efficacy that is comparable to optimal NT-3, but they have lower potency (EC₅₀ 2 nM for 2B7 and 8 nM for PTP-sigma, *versus* EC₅₀ 0.2 nM for NT-3). Mab **2F5** has significantly lower efficacy and potency. Alone, small molecules **3Aa** and **1Aa** have low potency and low efficacy, but respectively enhance the efficacy of 0.1 nM NT-3 from 24% to 65% and 71%, significant versus controls; two-tailed t-test. **B.** TrkC.T1 agonist induction of TNF α in rMC-1-TrkC.T1 cells. Shown are the bioactive agents, some of the inactive ligands are omitted. Data are mean \pm standard deviation. Symbols indicate significance * $p \leq 0.05$; two-tailed t-test.



Transparent Methods

Cell lines

Human embryonic kidney HEK 293 (female origin, ATCC) and mouse embryonic fibroblast NIH3T3 cells (ATCC) were transfected with plasmids encoding human full-length *TrkC* (293-TrkC-FL, NIH-TrkC-FL) or with human or rat *TrkC.T1* (293-rTrkC.T1, 293-hTrkC.T1, NIH-TrkC-T1) or with human *TrkC.T1*^{Δinsert} construct that was generated by transfection with a pcDNA6 blasticidin-resistant plasmid containing a PCR-generated amplicon encompassing amino acids 1 to 528 of human *TrkC.T1* (293-hTrkC-Δ-ICD). The rat glial cell line, rMC-1 has been previously characterized (Sarthy et al, 1998) and expresses low levels of endogenous *TrkC.T1*, and was also transfected with human *TrkC.T1* cDNA (rMC-1-TrkC.T1). Nnr5 cells are a variant of PC12 cells that lost expression of *TrkA* (the NGF receptor) and were stably transfected with *TrkC-FL* cDNA and express functional protein on the surface. Stably transfected cell lines were subcloned under drug selection (depending on the vector, 0.5 mg/ml G418, or 2 μg/ml puromycin, or 10 μg/ml blasticidin) and selected based on relatively high expression of receptors (100,000/cell, similar across all lines). Equal expression was verified by flow cytometry, by PCR, and by western blot using our own mAbs or commercial mAb C44H5 antibody that recognizes both isoforms (Cell signalling) (e.g. see (Brahimi et al, 2016)). Expression of the receptor levels indicated do not alter cell physiology since there is no significant ligand-independent activation (e.g. see **Figure 6D**, untreated cells), and in serum free conditions all cells die at the same rate as non-transfected cells. All cell lines were mycoplasma free and were regularly tested by using a PCR mycoplasma detection kit (Zentech).

Mice

The animal protocol used was reviewed and approved by the Lady Davis Institute Animal Care Committee and animal experiments were performed according to the guidelines of the Canadian Council on Animal Care. Healthy wild-type female Balb/c mice (10-12 weeks of age, 19-20g) were purchased from Charles River Laboratories (Montreal, Quebec, Canada) and used for the generation of monoclonal antibodies (mAbs). A maximum of five mice per cage were kept in a 12 hr dark-light cycle with food and water *ad libitum*.

Immunization and generation of mAbs

We generated mAbs that bind to *TrkC-FL* and/or *TrkC.T1*. One strategy was immunization of mice that do not express *TrkC.T1*, due to an engineered point mutation at the alternative splicing

site that generates TrkC.T1 mRNA from TrkC-FL mRNA (thereafter named “TrkC.T1 knockout”). The TrkC.T1 knockout mice do not produce TrkC.T1 mRNA or protein (Bai et al., 2010a). Wild type mice were also successfully immunized with live NIH3T3 mouse fibroblasts stably transfected with human TrkC.T1 cDNA (NIH-TrkC.T1), expressing high levels of protein on the cell surface (Brahimi et al, 2016). Other mice were immunized with peptides of the juxtamembrane region of TrkC (present in both TrkC-FL and TrkC.T1 (ESTDNFILFDEVSPPTPI) or the unique neopeptide of TrkC.T1 intracellular domain and only present in TrkC.T1 (GIYVEDVNVYFSKGRHG). All peptides were synthesized *in house* and conjugated to KLH as a carrier. Hybridomas were generated from serum-positive mice by fusion of B-cells with SP20 myeloma cells, using standard techniques. Hybridomas were screened in binding assays by IHC and by flow cytometry using cells stably transfected to express either TrkC-FL or TrkC.T1 (e.g. NIH-TrkC.T1 or NIH-TrkC-FL; 293-TrkC.T1 or 293-TrkC-FL), compared to controls wild type non-transfected cells and to cells transfected to express related receptors such as TrkA. The mAb 2B7 binds to the TrkC IgG-C2 (D5) domain (Guillemard et al., 2010). All mAbs were purified in protein G columns for use in binding and biological assays.

Biotinylation of NT-3.

NT-3 (Alomone Labs ProSpec) was biotinylated by incubating 2 μ M of NT-3 with 400 μ M of Sulfo-NHS-LC-Biotin (ThermoFisher scientific, cat # 21335) for 40 min at room temperature in PBS (20-fold molar excess of biotin reagent). Biotinylated NT-3 was concentrated, and unbound biotin removed, using a desalting Amicon Ultra-0.5 ml centrifugal filter (Ultracell:10K, Millipore).

Small molecules.

The synthesis and the bioactivity of small molecules **3Aa** and **1Aa** and their fluorescein-conjugated analogs (3Aa-FITC and 1Aa-FITC) have been described (Zaccaro et al, 2005). These agents are reported agonists of TrkC-FL and promote cell survival and cell differentiation.

Flow cytometry.

The ligands were tested by quantitative flow cytometry (Guillemard et al., 2010). Briefly, 293 or NIH-WT or expressing TrkC-FL or TrkC.T1 cells were resuspended in 0.1 mL of flow cytometry buffer and incubated with the indicated compounds for 30 min at 4°C, and washed three times to remove excess. For mAbs, secondary reagent was anti-mouse IgG conjugated to fluorescein. Cells were then suspended in buffer and analyzed by flow cytometry using Flowjo program. As negative controls, no primary (background fluorescence) or irrelevant mouse IgG were used. Reported are

the mean channel fluorescence (MCF) values of at least two independent experiments. For mild reduction tests, live cells were exposed to DTT (10 mM) for 10 min at room temperature. After washing once, iodoacetamide (15 mM) was added to prevent reformation of disulfide bonds, followed by a second wash. MAb 2B7 binding was then studied by flow cytometry, as described above.

Binding competition assays

Binding competition assays were performed (Guillemard et al., 2010; Barcelona et al, 2015) with agents (mAbs, small molecules, or PTP-sigma) tested as competing the binding of NT-3–biotin, or with NT-3 tested as competing the binding of mAbs, small molecules, or PTP-sigma. Cells expressing the indicated TrkC receptor were pre-incubated with competitor (50 nM to 5 μ M) for 15 min in PBS/0.2% BSA/0.1% Na Azide pH 7.3 (FACS buffer) at 4°C. Then, labeled binding agents were added (10 nM) for another 15 min. After a FACS buffer washing steps, cells were incubated with fluorescein-conjugated-secondary agent for 15 min at 4°C (for NT-3–biotin avidin-fluorescein (Sigma), and for the MAbs or PTP-sigma anti-Ig-fluorescein (Sigma)). No secondary was added for the small molecules, as they are directly labeled with a fluorescein molecule. After two washing steps, cells were analyzed immediately by flow cytometry. Mean channel fluorescence (MCF) values of bell-shaped histograms were standardized, with no competition = 100%, and secondary without primary = 0%. % of MCF values are the mean of three independent experiments \pm SD.

Fluorescence Microscopy.

Cells expressing TrkC-FL or TrkC.T1 were plated on coverslip. After 24 h, cells were exposed to 3Aa-FITC or 1Aa-FITC (10 μ M) for 30 min in flow cytometry buffer on ice. After a washing step, cells attached on coverslip were fixed, washed and mounted. Images were taken with a Leica DM LB 2 microscope equipped with the LAS acquisition software and a Leica DFC350 camera for detection, applying a 63x objective. Images were saved directly in TIF format and adjusted for unbiased brightness and contrast using Adobe Photoshop CS 8.0.

Immunohistochemistry.

Cryosections of WT mice or G93A ALS mice were immunostained with 1E11 mAb or 1B2 mAb and GFAP antibody (Cell Signaling, cat # 3670). Images were taken with a Leica DMI6000 B microscope equipped with the Quorum technologies WaveFX spinning disk confocal microscopy system, the Volocity software and a high dynamic Imagem EM-CCD camera for detection.

Pictures were acquired as Z-stacks of confocal optical sections applying a 63x objective. Images were exported directly in TIF format and adjusted for unbiased brightness and contrast using Photoshop CS 8.0.

Cell Metabolism/Survival functional assays.

The growth/survival profile of cells were quantified in 96-well plates using the tetrazolium salt reagent 4-[4,5-dimethylthiazol-2-yl]-2,5-diphenyltetrazolium bromide (MTT; Sigma) 48-72 hr after plating; by reading the optical density (OD) (Maliartchouk et al., 1997). NIH-TrkC-FL or 293-TrkC-FL cells were treated with different concentrations of the test agents, or with vehicle, or with NT-3 (positive control). Cells expressing a related receptor TrkA (and its ligand NGF) were used as cellular specificity control. Each individual assay was done in quadruplicate and was repeated n=3 independent times. MTT data were standardized to optimal dose of neurotrophin = 100% survival, and serum-free medium (SFM) = 0% survival, using the formula $[(OD_{\text{test}} - OD_{\text{SFM}}) \times 100 / (OD_{\text{optimal NTF}} - OD_{\text{SFM}})]$. Only optimal doses are shown, for simplicity, which correspond to 2 nM NT-3, 40 nM for mAbs, 10 μ M for small molecules, 35 nM for PTP-sigma.

Immunoprecipitation and Western Blot Analysis

Detergent lysates of cells expressing either TrkC-FL, TrkC- Δ -ICD or TrkC.T1 were immunoprecipitated with anti-pan-TrkC (C44H5, Cell Signaling, cat # 3376). Proteins were eluted from the protein G-agarose beads and resolved by SDS-PAGE in reducing (DTT) or non-reduced conditions. Membranes were blotted with anti-pan-TrkC or with two different anti-PDI mAbs (Cell Signaling, cat# 2446 and Genetex, RL90, cat# GTX22792). Mild reduction assays were performed in NP-40 detergent lysates prepared from 293-TrkC-FL or 293-TrkC.T1 cells. Cleared whole cell lysates were resuspended in SDS-PAGE Laemmli buffer lacking reducing agents. After 1 min of exposure to 90°C, DTT (10 mM) was added to the samples and incubated for 15 min at room temperature. All samples were resolved immediately by SDS-PAGE. After western transfer, membranes were immunoblotted with mAb 2B7 (TrkC-FL specific). Densitometric quantification was done using ImageJ software. * p<0.05, ** p< 0.01 versus control (n=3 independent experiments).

Biochemical signals

Cell signals were reduced to baseline by culture in minimal media for 2 hours. Then, optimal concentrations of NT-3 (2 nM) or PTP-sigma (35 nM) or control vehicle PBS were added and cells were collected after 0, 5, 12, 30 min of stimulation. Whole cell detergent lysates were prepared

and resolved by SDS-PAGE. After western blotting, membranes were studied with specific mAbs directed to the phosphorylated mediators pAkt (Cell Signaling, # 9271), pTrkC (Millipore, # 05-321), pErk1,2 (Cell Signaling, #4370); or against actin as standard control for loading (Sigma, #A2066). N = 3 assays with independently processed lysates. For simplicity, only relevant ligand concentrations and time-points are shown.

Differentiation Assays

Nnr5 cells are a variant of PC12 cells that lost TrkA expression but retain p75^{NTR} expression. Nnr5-TrkC-FL cells are stably transfected with TrkC-FL cDNA and express protein on the surface. The indicated treatments were added for 72 h and differentiation of adherent cells was scored morphologically as % of cells with neurites (> 2 cell body long). Quantification was done by image analysis, from at least two independent assays.

Upregulation of TNF α by activated TrkC.T1, in quantitative real-time PCR assays

Rat glial rMC-1 cells expressing TrkC.T1 were treated with the indicated agents for 6 hr: **3Aa** or **1Aa** (10 μ M), LPS (1 μ g/ml) (Shariff et al), NT-3 (2 nM) or mAbs (40 nM), human recombinant PTP-sigma ectodomain (10-50 nM) (R&D Systems 3430-PR-050). The mRNA was prepared from the cells using the qScript RNA cDNA synthesis kit (Quanta). Samples were used for real-time quantitative PCR with primers for rat TNF α and rat RNAs18 (Barcelona and Saragovi, 2015;Brahimi et al., 2016). Data are expressed as the mean \pm SEM relative to the untreated group (3 independent experiments, each in triplicate).

Mass spectrometry.

TrkC immunoprecipitates were digested with 6 μ l of proteomics-grade Trypsin (Promega) at a concentration of 12 ng/ μ l in 50 mM ammonium bicarbonate, overnight, at 37 °C. Digested peptides were washed off the beads with 200 μ l of water, the peptide digests were split into two 100 μ l aliquots and transferred to clean Eppendorf tubes. One of the Eppendorf tubes was supplemented with DTT (5 mM) and both tubes were heated to 55° C for half an hour. Subsequently, both tubes were supplemented with iodoacetamide (IAA, 10 mM) and after an hour samples were dried in a speed vacuum. The dried peptides were reconstituted in 25 μ l of water supplemented with 0.1% formic acid (FA) and transferred to a 200 μ l sample vial. The peptide samples were subjected to LC reverse phase nanoflow chromatography using a Proxeon Easy nLC (Thermo Scientific). The peptides were trapped onto a 2 cm C18 column (Acclaim PepMap 100, Thermo Scientific) and were separated at a flow rate of 350 nl/minute on a 15 cm C18 analytical

nanocolumn (Acclaim PepMap RSLC, Thermo Scientific) with a water/Acetonitrile gradient covering 3%-35% Acetonitrile over 100 min. The eluting peptides were analyzed by an Orbitrap Q-Exactive HF (Thermo Scientific) operating with a duty cycle of 25 MSMS fragment spectra per precursor scan. The resolution was set at 120,000 (scan speed 2 spectra per second) for precursor scans, over mass range of 375-1400 m/z, and 30,000 (scan speed 25 spectra per second) for fragment spectra. The mass spectrometer was operated with a dynamic exclusion set at 6 seconds and maximum trap fill. The acquired spectra were converted into Mascot Generic Files (mgf) using Mascot Distiller (Matrix Sciences) and searched against the Human proteome (Uniprot). Searches were performed using the Mascot proteomics search engine (Matrix Sciences), setting mass tolerance of 6 ppm for precursor ions and 50 mDa for MSMS ions and selecting Carbamidomethyl modification modifications of cysteines as a fixed modification and oxidized Methionine as a variable modification. The Mascot data output was transferred to Scaffold (Proteome Software) for data validation for peptides/proteins with a false discovery rate (FDR) of better than 5%.

Mass spectrometry data analysis

Scaffold v4.8.9 was used to extract the data set of trypsin-generated peptides detected by mass spectrometry in reducing and non-reducing conditions, as well as the coverage of each isoform of TrkC (TrkC.T1, TrkC-FL and TrkC- Δ -ICD). To gain further insights into the covalent structure of the ectodomain of each TrkC isoform, unique pairs of peptides were searched in the reduced conditions whose combined mass (AMU) matches that of peptides detected the non-reduced condition, with an error of up to 10 units. Peptides in reducing conditions were restricted to those whose sequences mapped to the extracellular domain of TrkC (residues 32-429 of NTRK3_HUMAN based on UniProtKB).

Quantification and statistical analysis

The dispersion and precision measures (mean \pm SD), the statistical significance and the exact value of “n” are reported in the Figures and Figure Legends. Differences between treated and untreated groups were assessed by two-tailed student t-test. For multiple groups, one-way ANOVA with Tukey-Kramer Multiple Comparisons Test compared different groups. Significance $p < 0.05$ (*), $p < 0.01$ (**) and $p < 0.001$ (***).

References for Supplemental and Methods

Barcelona, P.F., and Saragovi, H.U. (2015). A Pro-Nerve Growth Factor (proNGF) and NGF Binding Protein, alpha2-Macroglobulin, Differentially Regulates p75 and TrkA Receptors and Is Relevant to Neurodegeneration Ex Vivo and In Vivo. *Mol Cell Biol* 35, 3396-3408.

Brahimi, F., Maira, M., Barcelona, P.F., Galan, A., Aboukassim, T., Teske, K., Rogers, M.L., Bertram, L., Wang, J., Yousefi, M., *et al.* (2016). The Paradoxical Signals of Two TrkC Receptor Isoforms Supports a Rationale for Novel Therapeutic Strategies in ALS. *PLoS One* 11, e0162307.

Guillemard, V., Ivanisevic, L., Garcia, A.G., Scholten, V., Lazo, O.M., Bronfman, F.C., and Saragovi, H.U. (2010). An agonistic mAb directed to the TrkC receptor juxtamembrane region defines a trophic hot spot and interactions with p75 coreceptors. *Dev Neurobiol* 70, 150-164.

Maliartchouk, S., and Saragovi, H.U. (1997). Optimal nerve growth factor trophic signals mediated by synergy of TrkA and p75 receptor-specific ligands. *J Neurosci* 17, 6031-6037.

Sarthy, V.P., Brodjian, S.J., Dutt, K., Kennedy, B.N., French, R.P., and Crabb, J.W. (1998). Establishment and characterization of a retinal Muller cell line. *Invest Ophthalmol Vis Sci* 39, 212-216.

Zaccaro, M.C., Lee, H.B., Pattarawarapan, M., Xia, Z., Caron, A., L'Heureux, P.J., Bengio, Y., Burgess, K., and Saragovi, H.U. (2005). Selective small molecule peptidomimetic ligands of TrkC and TrkA receptors afford discrete or complete neurotrophic activities. *Chem Biol* 12, 1015-1028.